Available online at www.sciencedirect.com
SCIENCE DIRECT
Developmental Biology 290 (2006) 246 – 264
DEVELOPMENTAL BIOLOGY
www.elsevier.com/locate/ydbio

Cooperative non-cell and cell autonomous regulation of Nodal gene expression and signaling by Lefty/Antivin and Brachyury in *Xenopus*

Young Ryun Cha, Shuji Takahashi [1], Christopher V.E. Wright *

Department of Cell and Developmental Biology, Program in Developmental Biology, Vanderbilt University School of Medicine, 465 21st Avenue South, Nashville, TN 37232, USA

Received for publication 2 August 2005, revised 20 October 2005, accepted 28 October 2005
Available online 6 January 2006

Abstract

Dynamic spatiotemporal expression of the *nodal* gene and its orthologs is involved in the dose-dependent induction and patterning of mesendoderm during early vertebrate embryogenesis. We report loss-of-function studies that define a high degree of synergistic negative regulation on the *Xenopus nodal*-related genes (*Xnrs*) by extracellular *Xenopus antivin/lefty* (*Xatv/Xlefty*)-mediated functional antagonism and Brachyury-mediated transcriptional suppression. A strong knockdown of Xlefty/Xatv function was achieved by mixing translation- and splicing-blocking morpholino oligonucleotides that target both the A and B alloalleles of Xatv. Secreted and cell-autonomous inhibitors of Xnr signaling were used to provide evidence that Xnr-mediated induction was inherently long-range in this situation in the large amphibian embryo, essentially being capable of spreading over the entire animal hemisphere. There was a greater expansion of the Organizer and mesendoderm tissues associated with dorsal specification than noted in previous Xatv knockdown experiments in *Xenopus*, with consequent exogastrulation and long-term maintenance of expanded axial tissues. Xatv deficiency caused a modest animal-ward expansion of the marginal zone expression territory of the *Xnr1* and *Xnr2* genes. In contrast, introducing inhibitory Xbra-En^R fusion constructs into Xatv-deficient embryos caused a much larger increase in the level and spatial extent of *Xnr* expression. However, in both cases (Xatv/Xlefty-deficiency alone, or combined with Xbra interference), *Xnr2* expression was constrained to the superficial cell layer, suggesting a fundamental tissue-specific competence in the ability to express *Xnrs*, an observation with direct implications regarding the induction of endodermal vs. mesodermal fates. Our experiments reveal a two-level suppressive mechanism for restricting the level, range, and duration of Xnr signaling via extracellular inhibition by Xatv/Xlefty coupled with potent indirect transcriptional repression by Xbra.

Keywords: Morpholino; Xnr; Xlefty/Xantivin; Xbrachyury; Organizer; Mesendoderm induction; Gastrulation; *Xenopus laevis*

Introduction

Intercellular signaling via the TGFβ family member Nodal plays a central role in mesendodermal fate specification and patterning of vertebrate embryos (Schier, 2003; Schier and Shen, 1999; Whitman, 2001). Fundamental questions related to how the activity of this potent inducer is deployed during embryonic patterning include how it is regulated transcriptionally and post-transcriptionally, and how post-translational modifications affect protein secretion, ligand maturation from the pro-protein, or ligand movement characteristics within the extracellular milieu (Constam and Robertson, 1999; Le Good et al., 2005). Biological effects on the receiving cell also depend upon the availability of obligate receptor complex cofactors that are involved in signal receipt and transduction, such as the EGF-CFC proteins (Shen and Schier, 2000; Schier, 2003).

Little is known about whether the signals that initiate *nodal* expression are conserved across species, although links to maternally deposited inducers have been made in *Xenopus* and zebrafish (reviewed in Whitman, 2001; Schier, 2003). In several species, however, conserved *cis*-regulatory regions are beginning to be characterized that are involved in controlling later aspects of the maintenance and upregulation

* Corresponding author. Fax: +1 615 322 1917.
E-mail address: chris.wright@vanderbilt.edu (C.V.E. Wright).
[1] Present address: Department of Life Sciences (Biology), The University of Tokyo, 3-8-1 Komaba, Tokyo 153-8902, Japan.

0012-1606/$ - see front matter © 2005 Elsevier Inc. All rights reserved.
doi:10.1016/j.ydbio.2005.10.043

of expression of *nodal*/*nodal*-related genes. Among these, an important mechanism for maintaining and upregulating *nodal* expression during gastrulation stages, when anteroposterior and mesendodermal cell fates are being specified, involves a FAST/FoxH1-dependent Nodal autoregulatory loop (Norris and Robertson, 1999; Adachi et al., 1999; Osada et al., 2000; Pogoda et al., 2000; Saijoh et al., 2000). Such loops have an intrinsic property of tending to expand expression of the autoregulated gene through embryonic tissue, an effect that must be offset by negative feedback mechanisms in order to prevent inappropriate inductive effects. Well known examples of such feedback in other signaling systems include the induction of Ptc by Hh (Ingham and McMahon, 2001), and Dad by the *Drosophila* TGFβ-related molecule Dpp (Tsuneizumi et al., 1997).

An important extracellular feedback inhibitor of Nodal signaling is Lefty (also previously known as Antivin in frogs and zebrafish), whose transcription is directly activated by Nodal signaling (Meno et al., 1996, 1997, 1999; Bisgrove et al., 1999; Thisse and Thisse, 1999; Cheng et al., 2000; Tanegashima et al., 2000). Like Nodal, Lefty ligands are also released by protease cleavage from precursor pro-proteins (Sakuma et al., 2002). At the level of analysis carried out so far, Lefty is thought to work as a monomer to inhibit Nodal signaling at the level of the receptor complex, either by binding the EGF-CFC factor directly (Cheng et al., 2004; Tanegashima et al., 2004), or perhaps by physically interacting with the Nodal ligand itself (Chen and Shen, 2004). The idea that Lefty/Antivin is a key negative feedback regulator of *nodal/Xnr* expression fits well with their spatiotemporal expression characteristics. Loss-of-function experiments involving genetic manipulations in mice (Meno et al., 1999, 2001) or translational inhibition in frogs and zebrafish (Agathon et al., 2001; Chen and Schier, 2002; Feldman et al., 2002; Branford and Yost, 2002; Tanegashima et al., 2004) lead to increased and expanded Nodal signaling.

There is evidence from overexpression experiments in *Xenopus* and zebrafish that Lefty can move a long distance to suppress expression of Nodal-responsive genes in the marginal mesendodermal territory (Chen and Schier, 2002; Branford and Yost, 2002). Consistent with this idea, studies with mouse *Nodal*-GFP and *Lefty*-GFP fusion proteins in chicken embryos suggest that both ligands move relatively far, but that Lefty travels farther and faster than Nodal (Sakuma et al., 2002). The latter relationship is a tenet of reaction-diffusion models for inducer/antagonist signaling loops in embryonic patterning (Turing, 1952; Gierer and Meinhardt, 1972; Meinhardt and Gierer, 2000; Juan and Hamada, 2001; Chen and Schier, 2002). Because the relative level of Nodal signaling output arising from Nodal-Lefty (Xnr-Xatv/Xlefty) antagonism is likely to be a key determinant of cell fate, important goals include a full mechanistic description of the factors that affect the expression, diffusibility, and perdurance of Nodal and Lefty/Antivin in vivo.

The previous Xlefty/Xantivin (Xatv) loss-of-function studies in *Xenopus* (Branford and Yost, 2002; Tanegashima et al., 2004) showed less extensive effects on marker gene expression than those observed in zebrafish or mouse embryos. However, there was significant expansion in the expression of several mesendodermal markers, and of *Xnr2*, although the latter still remained relatively well restricted to the marginal zone region. The single antisense morpholino oligonucleotides (MOs) used in those papers targeted either the A or B copies (alloalleles) of *Xlefty/Xatv* that are found in this allotetraploid species. In our own studies, initiated before those papers were published, we reached similar conclusions regarding the effects of single MOs, but found variable phenotypes between batches of embryos, and thus became concerned with determining the effect of further reducing Xatv function by concurrently inhibiting both alloalleles. We report here that this manipulation produced a much more dramatic effect on downstream target gene activation and embryonic patterning, which was associated with an increased level and territory of *Xnr* expression and signaling. In agreement with previous studies, mesendodermal specification and patterning during early gastrulation in Xatv^{MO}-injected embryos began normally, but became greatly disrupted shortly thereafter. The abnormal embryonic morphogenesis was associated with very broad expansion of mesendodermal marker gene expression, including for example expansion of *Xbra* from the normal equatorial band to cover almost the entire animal cap region. A failure of involution combined with abnormal convergence/extension movements led to a form of exogastrulation, involving hyperdorsalization (over-specification of mesendodermal tissue), a morphant phenotype that is reminiscent of Xnr-induced hyperdorsalization. Our analysis provides stronger evidence that Xatv is a potent restrictor of the strength, duration, and range of Xnr signaling during the cell fate specification and patterning that occurs prior to and during gastrulation. Results with Xnr-selective inhibitors indicate that the massive expansion of the organizer and mesendodermal territory observed after Xatv knockdown was caused by large-scale increases in Xnr signaling range, which for certain genes extended to cover the entire animal hemisphere of this large embryo. These alterations of Xnr signaling during gastrulation caused enlargements of the mesendodermal tissues that were maintained in later stage embryos. Moreover, we found that the relatively small spatial expansion of *Xnr* expression in Xatv^{MO}-injected embryos is linked to an indirect transcriptional suppression from the expanded *Xbra* domain. The latter finding strongly supports the previous notion (Kumano et al., 2001) of a fundamental level of cross-regulation between Xbra and Xnr, but leads to a new understanding of the dual level regulation that ensures the transient and restricted nature of *Xnr* expression during gastrula stages. The expanded *Xnr2* expression domain in Xatv^{MO}- and/or Xbra-En^{R}-injected embryos is remarkably restricted to the superficial layer of the embryo, suggesting that the embryonic tissues exhibit a differential competence with respect to initiating the expression of essential regulatory genes such as the *Xnrs*. We present an integrated model for the multiple influences that cause the expression of *Xnrs* to be initiated and maintained in a narrow domain of the superficial marginal zone, which is a key determinant of their overall

inductive range for mesendodermal fate specification during gastrulation stages.

Materials and methods

Embryo manipulation and microinjections

Embryos were obtained by in vitro fertilization, de-jellied with 1% thioglycolic acid solution and cultured in 1× Steinberg's solution (SS; Kay and Peng, 1991) at 22°C, and staged according to Nieuwkoop and Faber (1967). Embryos were microinjected in 1× SS containing 5% Ficoll and then transferred and maintained in 1× SS. Capped mRNAs for microinjection were prepared using mMESSAGE mMACHINE (Ambion) according to the manufacturer's instruction with templates from the following linearized plasmids: pCS2+Xnr2 (Jones et al., 1995); pCS2+CerS (Piccolo et al., 1999); pSP64T-tALK4 (Chang et al., 1997); pSP64T-Xbra-En^{R} (Conlon et al., 1996); pCS2+nβgal; pBSKII-Xatv*. For inducing exogastrulation from normal embryos, vitelline membranes were removed from embryos at stage 8 and embryos were incubated in High Salt 1× SS (100 mM NaCl final concentration; all other components standard) until sibling embryos completed gastrulation. After high salt treatment, embryos were changed to 0.1× SS and collected at stage 25. Xatv^{MO}-injected embryos were incubated in 1× SS without vitelline membranes from stage 8 to the end of gastrulation and transferred to 0.1× SS until stage 25.

Morpholino oligonucleotides (MOs)

Xatv^{MO1} (5′-ACCCATTCTGATGTGACAGTCTACA-3′) was designed complementary to the region around the *Xatv* translational start site (Fig. 1A). Xatv^{MO2} (5′-AGGACTTGAAATACCTGCATTGCCC-3′) was generated from Xatv exon1/intron1 sequences determined from a genomic lambda phage clone using PCR (Fig. 1A); it is currently uncertain if Xatv^{MO2} is complementary to the pre-mRNA of both *Xatv^{A}/XleftyA* and *Xatv^{B}/XleftyB* alloalleles. The control morpholino was Gene Tools 'Standard' MO (5′-CCTCTTACCTCAGTTACAATTTATA-3′; human β-globin mutant sequence). The oligonucleotide sequence of XleftyB-MO was as previously reported (Branford and Yost, 2002; Fig. 1A).

In vitro translation

A plasmid construct, pCS2 + Xatv-2HA(B), was made from pCS2 + Xatv(B) by adding two HA-encoding sequences into downstream of the second cleavage site using quick change PCR site-directed mutagenesis (Stratagene). Originally, this construct was intended for Western blot assays to test efficiency of Xatv^{MO1} on exogenous Xatv translated in embryos, but the lack of HA signal led to its use in the in vitro translation assays.

Capped mRNAs were synthesized using mMESSAGE mMACHINE kit (Ambion). To try to ensure similar transcriptional/translational efficiencies, all cDNAs were placed into pCS2+. Xatv^{B} RNA was synthesized from pCS2 + Xatv-2HA(B). For mimicking Xatv^{A} RNA, pCS2 + Xatv-2HA(A) was constructed by adding 5 nucleotides into 5′-UTR of pCS2 + Xatv-2HA(B) using quick change PCR site-directed mutagenesis, resulting in the exactly same sequence as 5′-UTR of Xatv^{A}. Therefore, cDNAs of two Xatvs in plasmid constructs contain the same coding sequences (Fig. 1A). In vitro translation was performed as described (Taylor et al., 1996) with some modifications. Each RNA (1 μg) was mixed with 1 μg of the specified MO, heated to 70°C, slowly cooled to 37°C, then added to nuclease-treated rabbit reticulocyte lysate (Promega) with Redivue Pro-mix L-[^{35}S] labeling mix (>1000 Ci/mmol; Amersham) and incubated for 1 h at 30°C. *Xnr2* translation was used as a negative control.

Construction of Xatv cDNA*

The specificity of Xatv^{MO1} was tested by restoration of embryonic patterning by *Xatv* rescue cRNA (Xatv*). Quick-change PCR site-directed mutagenesis (Stratagene) was used on pBSKII-Xantivin (Xatv^{B}; Cheng et al., 2000) to delete/alter Xatv^{MO1}-target sequences in the 5′-UTR and coding region with oligonucleotides: 5′-GGCACTTGCACCCTGATGGGCGTCACTAC-CAAATC-3′; 5′-GATTTGGTAGTGACGCCCATCAGGGTGCAAGTGCC-3′ (ATG underlined; see Fig. 1A for final sequence of rescue RNA). Modifications were confirmed by sequencing. The specificity of the splicing blocker Xatv^{MO2} was shown by rescue with coinjected "wild-type" *Xatv* cRNA.

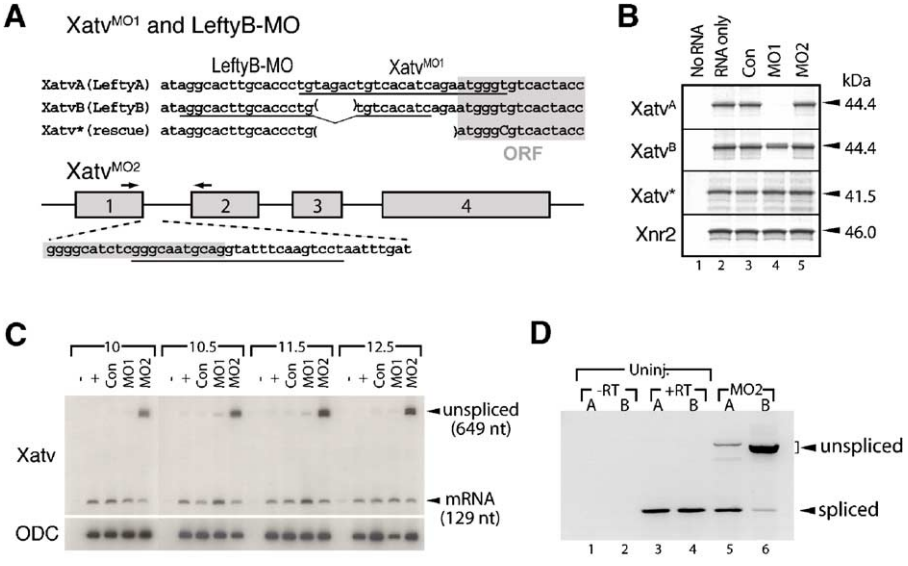

Fig. 1. Specific inhibition of *Xatv* translation and splicing with morpholino oligonucleotides. (A) Xatv MO positions relative to the translational start sites on *Xatv* mRNAs (Xatv^{MO1} and leftyB-MO) and the exon 1/intron 1 junction on *Xatv* genomic DNA (Xatv^{MO2}); see Materials and methods for actual MO sequences (reverse complements of those shown here). (B) Xatv^{MO1} inhibits the translation of *Xatv^{A}* in vitro. While translation of *Xatv^{A}* is completely inhibited by Xatv^{MO1}, *Xatv^{B}* translation is not blocked (lane 4). *Xatv** rescue RNA translation is not affected by Xatv^{MO1} (lane 4). Neither control MO nor Xatv^{MO2} affects translation of *Xatv* mRNAs (lanes 3, 5). Translation of *Xnr2* RNA is used as both loading control and negative control. (C) Xatv^{MO2} specifically inhibits *Xatv* pre-mRNA splicing (embryos received 50 ng of each Xatv^{MO} and were collected at the indicated stages). Primers in panel A (arrows) amplify across intron 1 using unspliced *Xatv^{A}* and *Xatv^{B}* pre-mRNA. (D) Xatv^{MO2} preferentially inhibits *Xatv^{B}* pre-mRNA splicing. Embryos injected with 50 ng of Xatv^{MO2} were collected at stage 10.5. RT-PCR was performed with A or B primer sets that amplify *Xatv^{A}* or *Xatv^{B}* pre-mRNA, respectively; see Materials and methods for primer sequences.

Whole-mount in situ hybridization and lineage tracing

Whole-mount in situ hybridization was performed as described (Sive et al., 2000). Embryos were fixed with 1× MEMFA (1 h). Some fixed embryos were embedded in 2% low melting agarose and bisected before or after in situ hybridization with a razor blade. Antisense probes were synthesized using Dig-labeling kit (Roche) from linearized plasmids: pBSK-Xnr2 (Jones et al., 1995); pBSKII-Gsc (Cho et al., 1991); pCS2+Chordin (Sasai et al., 1994); pCR-Script-ADMP (Moos et al., 1995); pCS2+Cer (Piccolo et al., 1999); pBSKII-XAntivin (Cheng et al., 2000); pXT1-Xbra (Smith et al., 1991); pBS-Derrière (Sun et al., 1999); pCS2+XWnt8 (Sokol et al., 1991); pT7Blue-3-Mixer (Henry and Melton, 1998); pSTBlue-1-Sox17α (Hudson et al., 1997); pBSKS-nrp-1 (Richter et al., 1988); pBSKS-cpl-1 (Richter et al., 1988); pBSKS-otx2 (Blitz and Cho, 1995); pBS-Xkrox20 (Bradly et al., 1993); pfhh4-Shh (Ruiz i Altaba et al., 1995); pBS-Edd (Sasai et al., 1996); pBSKS-MyoD (Hopwood et al., 1989). Hybridization was revealed using alkaline phosphatase conjugated to anti-digoxigenin Fab fragments (Roche) and BM purple (Roche) as color substrate. For lineage tracing, embryos were coinjected with *nuclear β-galactosidase* cRNA (250 pg or 400 pg), fixed with 1× MEMFA, and visualized with coloration using 6-chloro-3-indolyl-β-D-galactoside (Red-Gal; Research Organics).

RT-PCR

Total RNA was isolated using TRIzol (Invitrogen), and cDNA synthesis and PCR were performed as described (Wilson and Melton, 1994). Trace [^{32}P]-dATP-radiolabeled PCR products were resolved on 5% non-denaturing polyacrylamide gels. PCR primers and cycle numbers were as described for *ornithine decarboxylase* (ODC), *Xatv* (Agius et al., 2000; Cheng et al., 2000). The unspliced fragment of *Xatv* RNA caused by Xatv^{MO2} was detected by PCR with 5′-TCTATGCTGCACAATCACAGA-3′ (forward) and 5′-GGACTGCTT-GCTGGAGTCTGA-3′ (reverse); 25 cycles. Conditions in which Xatv primer pairs amplified in the linear range were empirically determined. For non-radioactive RT-PCR to analyze Xatv^{MO2} specificity against *Xatv^A* or *Xatv^B* pre-mRNA, the following primers were used with 34 cycles: 5′-ATACATGT-CTATGCTGCACAG-3′ (Xatv^A forward), 5′-CTCCATTCCAAAGACCA-TGGT-3′ (Xatv^A reverse), 5′-GTACATGTCTATGCTGCACAA-3′ (Xatv^B forward), 5′-CTCCATTCCAAAAACCAGGGA-3′ (Xatv^B reverse). The PCR primers for *Xnr1*, *Xnr2*, *Xnr4*, *Xnr5*, and *Xnr6* were described by Takahashi et al. (2000).

Histology and statistics

Histological analysis was performed as described in Cheng et al. (2000), except using Histo-clear (National Diagnostics) instead of toluene. After transverse section of three high salt (HS)- or Xatv^{MO}-induced exogastrulae, seven serial sections per each exogastrulae were selected from the middle region of the mesendodermal mass with respect to the A/P axis. Areas of notochord or somite from whole exogastrulae were determined by weighing prints of the digital images and expressed as mean percentage ± SE. Significance of the tissue area alterations between HS- and Xatv^{MO}-induced exogastrulae used the unpaired *t* test.

Results

Morpholino-based inhibition of translation and splicing of Xenopus Lefty/Antivin

We adopted a morpholino oligonucleotide-based approach to block the function of both Xatv^A and Xatv^B alloalleles, concurrently, to gain a full appreciation of the role of Xatv in limiting Xnr signaling range during *Xenopus* embryogenesis. A translation-inhibiting MO, Xatv^{MO1}, was designed from 5′-UTR and translational initiation sequences present in 24 gastrula stage Xatv cDNAs (Cheng et al., 2000) of the A and B alloalleles (at approximately 2:1 ratio). The two alleles have previously been referred to as *Xlefty A* and *Xlefty B* (Branford et al., 2000; Fig. 1A). The 25 nt Xatv^{MO1} matches Xatv^A over its entire length and Xatv^B over the first 18 nt of the MO 5′ end (Fig. 1A). The current understanding of MO function (GeneTools Inc., technical advice) suggests that Xatv^{MO1} should suppress translation of *Xatv^A* and *Xatv^B* mRNAs. However, Xatv^{MO1} failed to block in vitro translation of *Xatv^B* cRNA under conditions that effectively blocked *Xatv^A* translation (Fig. 1B, lane 4). Translation of the rescue RNA *Xatv** (Fig. 1A) used in the specificity tests below was not affected by Xatv^{MO1} (Fig. 1B, lane 4). Translation of *Xnr2*, a negative control, was not affected by any Xatv^{MO} that we tested (Fig. 1B), and the GeneTools control MO did not affect translation of any RNA. Concerns that the unbound 3′ tail of Xatv^{MO1} might facilitate its displacement from *Xatv^B* mRNAs (e.g., by scanning ribosomes), or that structural features of *Xatv^B* mRNA somehow render it refractory to inhibition by certain MOs (usually ~25% of failure rate in the first MO; personal communication with GeneTools Inc.), and problems with the knock-down efficiency of other *Xatv^B*-specific MOs, led us to synthesize another MO, Xatv^{MO2}, to target the splicing of *Xatv^B* pre-mRNA at the exon1/intron1 junction (Fig. 1A).

The splice blocker Xatv^{MO2} did not reduce translation of *Xatv^A* or *Xatv^B* RNA (Fig. 1B, lane 5). The efficacy of splicing blocking by Xatv^{MO2} was assessed by RT-PCR using primers to amplify across intron 1 (Fig. 1A) of both *Xatv^A* and *Xatv^B* on template RNA extracted from Xatv^{MO2}-injected (50 ng, 1-cell stage) gastrula stage embryos. This method detects spliced and unspliced RNA without regard for its derivation from *Xatv^A* and *Xatv^B*. While spliced RNA was still detected, substantial unspliced pre-mRNA was detected in Xatv^{MO2}-injected embryos compared to controls (Fig. 1C). The aggregate amount of [unspliced + spliced] RNAs was increased compared to controls, likely related to enhanced *Xatv* expression induced by the increased Xnr signaling in the Xlefty/Xatv-deficient situation (see below), with perhaps some contribution from MO-induced mRNA stabilization. Next, to analyze the selectivity of Xatv^{MO2} against splicing of RNA from the *Xatv^A* or *Xatv^B* alloallele, RT-PCR was performed with primers designed based on cDNA sequences that are selective for *Xatv^A* or *Xatv^B* RNA. *Xatv^A* and *Xatv^B* RNAs were expressed at similar levels in normal embryos, consistent with previous reports (Fig. 1D, lanes 3 and 4; Branford et al., 2000). In Xatv^{MO2}-injected embryos, however, spliced PCR products are mostly *Xatv^A*-class (Fig. 1D, lane 5). *Xatv^A* mRNA splicing was blocked to a small degree, as indicated by the presence of the slightly larger “unspliced” DNA fragment compared to *Xatv^B* (Fig. 1D, lane5); whether this is because there is increased Xatv/Xlefty expression because of the increased Xnr signaling is currently unknown. There was, in contrast, a major effect on *Xatv^B* splicing (Fig. 1D, lane 6). The selective effect of Xatv^{MO2} on *Xatv^B* splicing was confirmed by testing the PCR products generated in the same way as Fig. 1C for cleavage by *Xatv^B*-specific restriction enzymes, chosen from *Xatv^B* exon and intron sequence (the *Xatv^A* intron sequence is not available yet). In pilot experiments, they did not cleave

intron-spanning DNA fragments made by RT-PCR with $Xatv^A$-specific intron-flanking primers (data not shown). Overall, these data demonstrate that $Xatv^{MO1}$ mainly inhibits translation of $Xatv^A$ mRNA, and that $Xatv^{MO2}$ selectively and efficiently targets the splicing of $Xatv^B$ pre-mRNA.

Overall embryonic defects and specificity of $Xatv^{MO}$ function

We first compared the *Xatv* loss-of-function phenotype after injecting $Xatv^{MO1}$, $Xatv^{MO2}$, or both mixed together at the 1-cell stage (Fig. 2A). Experimental embryos scored at late

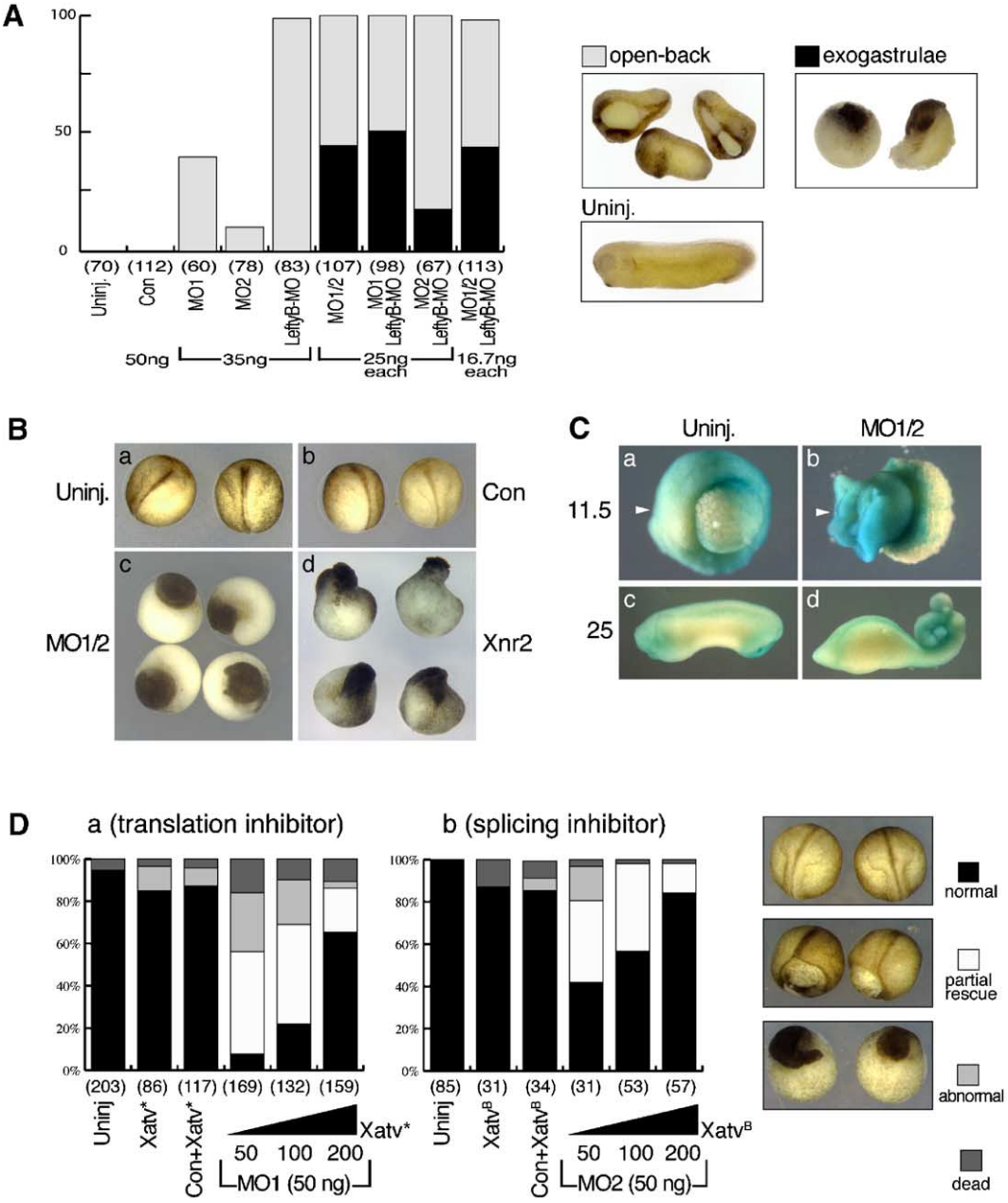

Fig. 2. Loss of Xatv function causes gastrulation defects. (A) Synergistic targeting by coinjection of $Xatv^{MOs}$. Coinjection of lower dose (25 ng or 16.7 ng each) of each $Xatv^{MO}$ that targets both $Xatv^A$ and $Xatv^B$ RNA ($Xatv^{MO1}$ + leftyB-MO, $Xatv^{MO1}$ + $Xatv^{MO2}$ and $Xatv^{MO1}$ + $Xatv^{MO2}$ + leftyB-MO) is much more potent at knocking down Xatv function than single injection of each $Xatv^{MO}$ (35 ng). Coinjection of $Xatv^{MO2}$ and leftyB-MO (complementary to 5′-UTR of $Xatv^B$ mRNA; Branford and Yost, 2002) that mainly inhibit $Xatv^B$ function is less effective than coinjection of other MO combinations. (B) Compared to (a) uninjected embryos or (b) embryos receiving 50 ng of control MO at 1-cell stage, severe morphogenetic defects at neurula stage (St. 18) are caused by (c) 25 ng each $Xatv^{MO1}$ and $Xatv^{MO2}$ (45%, n = 42), or (d) 20 pg of *Xnr2* RNA (91.5%, n = 57). (C) Xatv depletion gives rise to exogastrulation. After 1-cell stage embryos received 30 ng each of $Xatv^{MO1}$ and $Xatv^{MO2}$, the vitelline membrane was removed at St. 9. (a) Uninjected embryo at St. 11.5. (b) Exogastrula caused by $Xatv^{MO1\,+\,MO2}$ injection at St. 11.5 (n = 10/10). (c, d) Uninjected (c) and $Xatv^{MO1\,+\,MO2}$-injected (d) embryo at St. 25. White arrowheads indicate the distal ectodermal region. (D) Xatv overexpression dose-dependently rescues the morphogenetic defects induced by $Xatv^{MO}$. (a) Rescue of $Xatv^{MO1}$ phenotypes by coinjection with the rescue RNA, *Xatv** (Fig. 1A). $Xatv^{MO1}$ (50 ng) was injected into 1-cell stage embryos with *Xatv** RNA (increasing pg dose indicated) and morphological changes scored at St. 18. *Xatv** alone (200 pg), or control MO (50 ng) together with *Xatv** (200 pg) did not significantly affect embryo development. In contrast, morphological defects caused by $Xatv^{MO1}$ injection were rescued by Xatv*, dose-dependently. (b) Dose-dependent rescue of splicing-blocker $Xatv^{MO2}$ phenotypes by coinjection with wild type $Xatv^B$ RNA (other experimental conditions as above).

neurula to tailbud stages displayed a spectrum of defects from severe gross exogastrulation, through a typical phenotype associated with abnormal gastrulation – an "open-back" defect in which the neural plate is split open – and down to almost normal tailbud morphology. Individual MOs caused a relatively low incidence of exogastrulation at the 50 ng dose (Xatv^{MO1}: 12%, n = 32; Xatv^{MO2}: 23%, n = 44). We tested whether concurrently blocking the function of Xatv^{A} and Xatv^{B} shifted the proportional representation of defects towards the more severe phenotype. The 35 ng dose of each individual MO produced a high incidence of open-back embryos. A mixture of a lower amount (25 ng each) of Xatv^{MO1} + Xatv^{MO2} induced a high proportion of exogastrulae (Fig. 2A). For unknown reasons, the Xatv^{MO2} splice blocker alone induced the open-back phenotype at a lower incidence than the Xatv^{A} translation blocker Xatv^{MO1} alone. A similar increase in effectiveness of Xatv^{MO1} + Xatv^{MO2} coinjection was seen by analyzing the expansion of mesendodermal marker expression (Figs. 3A: c, d, 4A: g–l; Supplemental Fig. 1A) in which *Xnr2*, *Gsc*, *Xatv*, and *Xbra* expressions were more expanded than in single MO injection. These data indicate a strong synergistic effect caused by simultaneously targeting *Xatv^{A}* and *Xatv^{B}* RNAs. During our studies, another report on MO-based loss-of-function of Xlefty was published by Branford and Yost (2002), who used XleftyA- or XleftyB-specific MOs in single injections. We synthesized XleftyB-MO and compared it alone, or in various mixtures with our MOs, to assess the knockdown effects. The 25 nt XleftyB-MO exactly matches the 5′-UTR of *Xatv^{B}* mRNA (Fig. 1A), and *Xatv^{A}* over 17 nt at the MO's 3′ end with a gap of 6 nt mismatch and 2 end matches. Like the single injection of Xatv^{MO1} or Xatv^{MO2}, no exogastrulae were caused by 35 ng of XleftyB-MO, although it caused ~100% incidence of the open-back phenotype (Fig. 2A). In contrast, combinations of MOs produced exogastrulae. Furthermore, the exogastrula incidence was higher in MO combinations that inhibit Xatv^{A}/Xatv^{B} together than for Xatv^{MO2}/XleftyB-MO mixtures that mainly target only Xatv^{B} (Fig. 2A). The incidence of the exogastrula by MO combinations that inhibit *Xatv^{A}/XleftyA* and *Xatv^{B}/XleftyB* together is comparable to that obtained by injecting approximately 70 ng of one Xlefty-MOs (40%; see Branford and Yost, 2002). The general view from marker analysis, however, suggested that combination MO-based loss of function of *Xatv^{A}* and *Xatv^{B}* caused much more profound effects on embryonic patterning than those targeting either alloallele. First, the expanded expression of specific markers, such as Xatv, was greater with *Xatv^{A}* and *Xatv^{B}* mixed MOs (e.g., Supplemental Figs. 1B: d, e), and the expansion was more reproducible across batches of embryos, with at least a 17–30% higher incidence of expanded *Xatv* in MO combinations that inhibit both alloalleles than in *Xatv^{B}*-targeting Xatv^{MO2}/XleftyB-MO mixtures (Supplemental Fig. 1B). Equal amount mixtures of (Xatv^{MO1} + Xatv^{MO2} + XleftyB-MO) had the same phenotype spectrum as for (Xatv^{MO1} + Xatv^{MO2}). Overall, the simple conclusion from these data is that a stronger inhibition of Xatv function is accomplished by simultaneous functional knockdown of both *Xatv^{A}* and *Xatv^{B}* RNAs. The more reproducible and larger scale phenotypic and marker gene

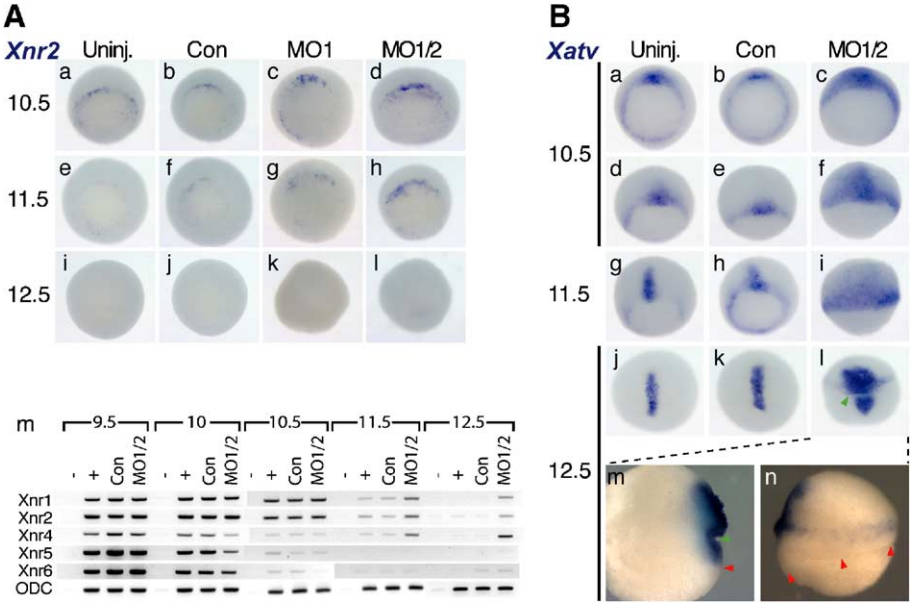

Fig. 3. Xatv depletion increases and prolongs *Xnr* expression levels and Xnr signaling. (A) Xatv$^{MO1 + MO2}$-injection upregulates and maintains *Xnr1* and *Xnr2* expression during gastrulation. (a–l) In situ hybridization (vegetal pole views) with *Xnr2* in (a, e, i) uninjected or (b, f, j) control MO (60 ng)-injected embryos compared to those injected with (c, g, k) Xatv^{MO1} alone (60 ng). [Quantitative analysis of alterations shown: c, n = 5/5; g, n = 6/6; k, n = 8/8.] (d, h, l) Xatv$^{MO1 + MO2}$ (30 ng each; quantitation: d, n = 14/15; h, n = 10/13; l, n = 13/13). Note the stronger *Xnr2* signal in Xatv$^{MO1 + MO2}$-injected embryos than in Xatv^{MO1}-injected embryos. (m) RT-PCR with total RNA from whole embryos injected with 60 ng control MO, or 30 ng of each Xatv^{MO1} and Xatv^{MO2} (– RT, + RT controls are from uninjected embryos). (B) *Xatv* expression is increased and expanded in Xatv$^{MO1 + MO2}$-injected embryos during gastrulation. (a–c) Vegetal views. (d–l) Dorsal views. [Quantitation: c, n = 13/15; i, n = 21/23, l, n = 13/15.] (m, n) Xatv$^{MO1 + MO2}$-injected embryos at St. 12.5 were bisected longitudinally through the center of the *Xatv* expression domain after whole-mount in situ hybridization and viewed either (m) internally or (n) externally (green arrowheads, indentation of the superficial layer (see text); red arrowheads, epiboly margin).

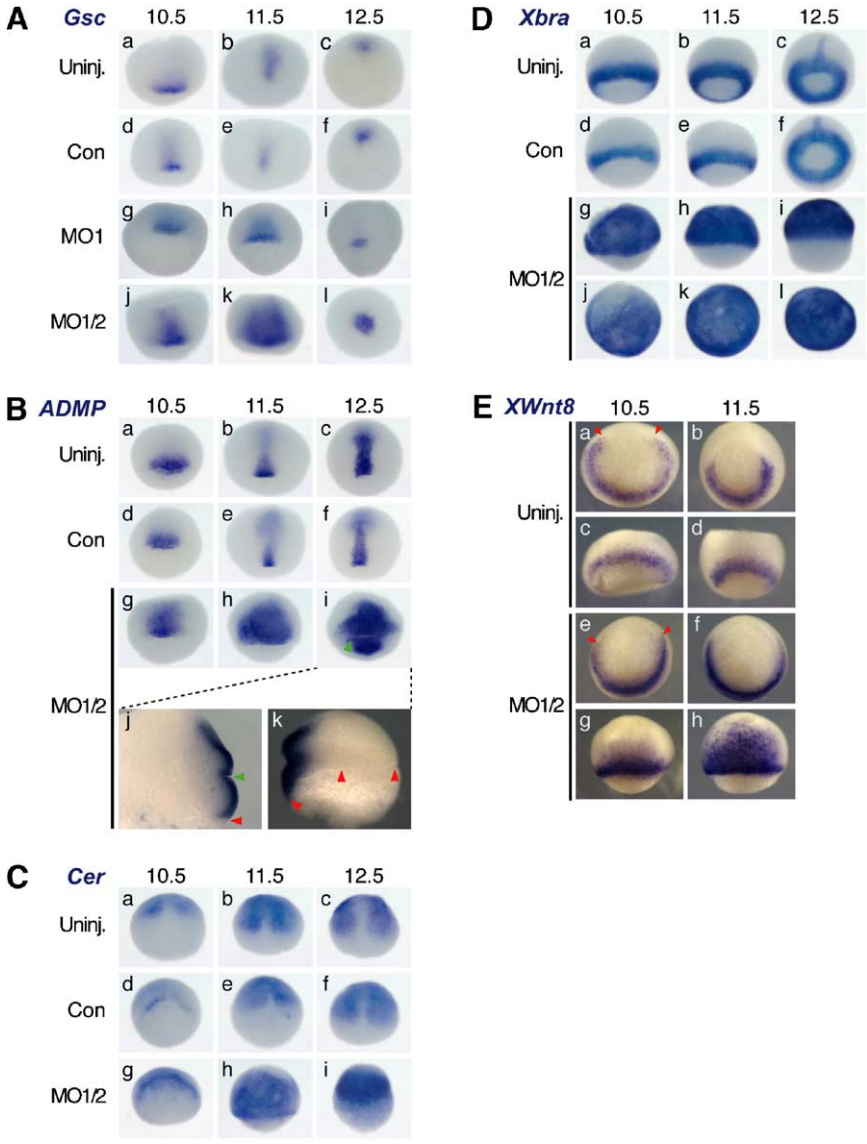

Fig. 4. Xatv is essential for normal organizer and mesoderm formation during gastrulation. 1-cell stage embryos received 60 ng of control MO, Xatv^{MO1}, or 30 ng each (Xatv^{MO1} + Xatv^{MO2}), and were assayed by in situ hybridization at the stages indicated. (A) *Gsc* expression. (a–l) Dorsal views. [Quantitative analysis of alterations shown: g, n = 9/9; h, n = 13/14; i, n = 9/9; j, n = 12/18; k, n = 13/14; l, n = 15/15.] Note the stronger and more expanded *Gsc* expression in Xatv$^{MO1 + MO2}$-injected embryos than in Xatv^{MO1}-injected embryos. (B) *ADMP* expression. (a–i) Dorsal views [Quantitation: g, n = 11/16; h, n = 15/17; i, n = 14/16.] (j, k) Xatv$^{MO1 + MO2}$-injected embryo at St. 12.5 was bisected through the center of *ADMP* expression domain along the animal–vegetal axis after in situ hybridization; lateral views are (j) internal or (k) external (green arrowheads, indentation of the superficial layer; red arrowheads, epiboly margin). (C) *Cer* expression. (a, d, g) Vegetal views. (b, c, e, f, h, i) Dorsal views. [Quantitation: g, n = 5/6; h, n = 7/7; i, n = 6/7.] (D) *Xbra* expression. (a–i) Lateral views, except panels c and f (vegetal views). (j–l) Animal views. [Quantitation: j, n = 14/15; k, n = 16/17; l, n = 15/17.] *Xbra* expression is massively expanded in Xatv$^{MO1 + MO2}$-injected embryos during gastrulation. (E) *XWnt8* expression. (a, b, e, f): Vegetal views, (c, d, g, h): Same embryos viewed ventrally. [Quantitation: e, n = 13/19; f, n = 11/15.] Red arrowheads show the arc of *XWnt8* non-expressing dorsal region.

expression alterations caused by the Xatv^{MO1}/Xatv^{MO2} mixture led to its use for the experiments described below.

Next, we analyzed morphological changes in Xatv$^{MO1 + MO2}$-injected embryos. Compared to uninjected embryos, MO-injected embryos (either Xatv$^{MO1 + MO2}$ or control MO) were approximately 30–40 min delayed in initiating formation of the dorsal lip (data not shown), but from stage 10.5 onwards, control MO and uninjected embryos had indistinguishable rates of development. The great majority of Xatv$^{MO1 + MO2}$-injected embryos developed very similarly to control embryos until stage 10.5, forming an incipient dorsal lip and initial blastopore groove. As reported previously (Branford and Yost, 2002), lateral spreading of the blastopore lip stopped fairly abruptly at stage 10.5, and gastrulation movements were effectively aborted. At stage 18, the severely disrupted embryos lacked a proper dorsoventral or anteroposterior axis (Fig. 2B: c), somewhat similar to that caused by Xnr2 overexpression (Fig. 2B: d). Culturing of Xatv$^{MO1 + MO2}$-coinjected embryos when unconstrained by the vitelline membrane allowed a form of exogastrulation (Fig. 2C: b, d; also see Branford and Yost, 2002).

The Xatv^{MO} phenotype was specifically attributable to decreased Xatv function. When Xatv^{MO1} was injected into 1-

cell embryos along with increasing doses of *Xatv** RNA (the 18 nt matching with Xatv^{MO1} was deleted, plus mismatches introduced; Fig. 1A), the phenotype was progressively rescued, leading to high proportions of normal embryos when scored at late neurula stage (Fig. 2D: a) or later (not shown). We note that the pBluescript-derived *Xatv** RNA is likely relatively inefficiently translated than when produced from other vectors, and *Xatv** did not cause a global embryonic phenotype in injected normal embryos. Because Xatv^{MO2} inhibits *Xatv* splicing but not translation (Fig. 1B, C), normal *Xatv* cRNA should overcome the defects caused by Xatv^{MO2}. Wild type *Xatv* RNA dose-dependently rescued the defects caused by Xatv^{MO1} (data not shown) and the splicing blocker Xatv^{MO2} (Fig. 2D: b).

Xatv depletion increases and prolongs Xnr expression

To characterize further the role of Xatv in regulating Xnr signaling, we examined the expression patterns of various markers, including Xnrs themselves, in Xatv$^{MO1 + MO2}$-injected embryos during gastrulation. We confirmed the previous results (Branford and Yost, 2002) with single MO injections (~50 ng), of a relatively modest effect on pan-mesodermal or region-specific (e.g., organizer) markers. In contrast, coinjection of Xatv$^{MO1 + MO2}$ (25–30 ng each) into 1-cell embryos produced more dramatic alterations (Figs. 3A, 4A; Supplemental Fig. 1A). Because Xatv is thought to be a feedback inhibitor of Xnr autoregulation, we first examined the expression of the *Xnr* genes that are expressed in a localized manner during gastrulation and have been determined to be largely affected by intercellular Xnr signaling (Jones et al., 1995; Joseph and Melton, 1997; Takahashi et al., 2000). By RT-PCR (Figs. 3A: m) and whole-mount in situ analysis (*Xnr2*, Fig. 3A; *Xnr1*, Supplemental Fig. 2), expression of both genes became upregulated starting at around mid-gastrula stage, with noticeably increased transcript levels maintained during gastrulation. Together with the elevated expression level, Xatv depletion induced, as previously reported (Branford and Yost, 2002), a modest expansion towards the animal pole of the domain of *Xnr1* and *Xnr2* expression (Fig. 3A: a–d, 8C, C′; see Supplemental Fig. 2 for *Xnr1*; note that *Xnr1* transcripts are more difficult to detect and record than other *Xnr* genes). A significant difference in the level of *Xnr* (Fig. 3A: m) and Xnr-responsive gene expression from the mid-gastrula stage (Supplemental Fig. 1A) suggests that Xatv negative feedback regulation, even during relatively early gastrulation, is critical for achieving an appropriate level of Xnr signaling. Among the four remaining *Xnr* genes, *Xnr5* and *Xnr6* are primarily activated by maternal factors and not by intercellular Xnr signaling (Takahashi et al., 2000; Yang et al., 2002; Rex et al., 2002). Indeed, RT-PCR assays showed that the expression levels of both of these genes were unaffected during both blastula and gastrula stage (Fig. 3A: m). The expression level of *Xnr4*, which is maintained by intercellular Xnr signaling (Joseph and Melton, 1997; Agius et al., 2000), was unaffected in the Xatv$^{MO1 + MO2}$-injected embryos until stage 10.5 (Fig. 3A: m). At stage 11.5, however, *Xnr4* showed a large increase compared to controls (Fig. 3A: m), likely related to its expression in axial midline tissue, which as described below is increased in Xatv$^{MO1 + MO2}$-injected embryos (Fig. 6). *Xnr3* expression was not analyzed as it is not currently thought of as a significant mesendodermal inducer, and is linked to Wnt-based patterning influences.

An important aspect that has, so far, not been studied in depth is the level to which the expression of *Xatv/Xlefty*, which is a direct target of Xnr signaling (Cheng et al., 2000; Tanegashima et al., 2000), is affected when Xatv translation is reduced. The level of *Xatv* expression was not changed at late blastula stage (stage 9.5; Supplemental Figs. 1A: i–l), but the dorsally disposed expression domain became greatly expanded during gastrulation, including a large animal pole-ward expansion (Fig. 3B; Supplemental Figs. 1A: m–t). The highly abnormal convergence/extension and involution movements in Xatv$^{MO1 + MO2}$-injected embryos were associated with a failure to narrow *Xatv* expression to the dorsal midline (Fig. 3B: i, l). At late gastrula (stage 12.5), the expression domain remained widespread and extended more vegetally in Xatv$^{MO1 + MO2}$-injected embryos (Fig. 3B: l). The observation that the *Xatv* expression domain is much broader than seen at any stage of normal control embryonic development indicates a true expansion of the expression domain rather than simply a MO-induced stabilization of *Xatv* mRNA. The impression of a dorsal lip margin (green arrowheads; Fig. 3B: l, m) was found to represent an indentation of the superficial cell layer, with the vegetal limit of *Xatv* expression (red arrowheads; Fig. 3B: m, n) representing the epiboly margin, and reflecting the lack of involution of the superficial region.

Spatiotemporal regulation of Xnr signaling by Xatv is essential for organizer/mesendoderm formation and convergent extension

The consequences of upregulated and maintained *Xnr* expression in Xatv$^{MO1 + MO2}$-injected embryos during gastrulation were examined further by analyzing additional Xnr-responsive genes. The expression patterns of the trunk organizer markers *chordin* (*Chd*; Sasai et al., 1994) and *Anti-dorsalizing morphogenetic protein* (*ADMP*; Moos et al., 1995), and the prospective prechordal plate organizer marker *goosecoid* (*Gsc*; Cho et al., 1991) were initiated normally at the onset of gastrulation (data not shown), but were upregulated in Xatv$^{MO1 + MO2}$-injected embryos at stage 10.5 (Figs. 4A, B; Supplemental Figs. 3A, C, G, K). In addition, the expression domains of these genes were greatly expanded into the animal/dorsal area from the mid-gastrula stage onward (Figs. 4A: k, B: h; Supplemental Figs. 3D, L). Consistent with the morphogenetic defects deduced from the abnormal *Xatv* expression pattern, there was no internalization or anterior-ward shifting of the *Gsc* and *Chd* expression domains (Fig. 4A: l; Supplemental Figs. 3D, L). In particular, *ADMP* expression remained, like *Xatv*, broad and non-internalized, with a morphological superficial indentation (green arrowheads; Figs. 4B: i, j) and vegetally extended epiboly margin on the dorsal side (red arrowheads; Figs. 4B: j, k). The head organizer marker *Cerberus* (*Cer*; Bouwmeester et al., 1996) was upregulated

and expanded by Xatv$^{MO1 + MO2}$-injection, although remaining dorsally disposed (Fig. 4C). In control embryos, a *Cer*-negative anterior midline domain corresponds to the anteriorly protruding (*Gsc*-expressing) prospective prechordal plate (Figs. 4C: a–f). In Xatv$^{MO1 + MO2}$-injected embryos, such a horseshoe-shaped *Cer* expression pattern was not observed. Substantial *Cer* expression was detectable in the subepithelial layer at the dorsal lip at stage 10.5, and *Cer* expression remained broadly expanded and adjacent to the epiboly margin over the next stages of gastrulation (Figs. 4C: g–i; data not shown). Because *Cer* is a downstream target of Nodal signaling, these observations are consistent with the idea that the relative balance between trunk and head tissues (Piccolo et al., 1999) is modulated by the action of Xatv on Xnr signaling.

Depleting Xatv function had a massive effect on the expression domains of *Xbrachyury* (*Xbra*), a pan-mesodermal marker (Smith et al., 1991), and *XWnt8*, a ventral mesodermal marker (Christian et al., 1991; Smith and Harland, 1991). Unlike the previous reports (Branford and Yost, 2002; Tanegashima et al., 2004) and our results with single MO injections (Supplemental Figs. 1A: f, g), Xatv$^{MO1 + MO2}$ together caused an enormous expansion of *Xbra* expression and, in most embryos, it covered almost the entire animal area, an effect that was maintained throughout gastrulation (Figs. 4D: g–l). In Lefty^{MO}-injected zebrafish embryos, the expression territory of the *Xbra* homolog *no tail* (*ntl*) expression was expanded by blastula (Agathon et al., 2001; Chen and Schier, 2002). In contrast, *Xbra* expression in late blastula stage Xatv$^{MO1 + MO2}$-injected embryos (as was seen for *Xatv*) was similar to control embryos (Supplemental Figs. 1: a–d), with expansion only beginning from the early gastrula stage (Fig. 4D; Supplemental Figs. 1A: e–h). Similarly, the expression of *XWnt8* was intensified in the ventrolateral marginal zone at stage 10.5, while the arc of dorsal non-expression was increased in size (red arrowheads; Figs. 4E: a, e), complementing the expansion of organizer markers described above. At mid-gastrula stage, *Xwnt8* expression covered the ventrolateral animal quadrant of Xatv$^{MO1 + MO2}$-injected embryos (Figs. 4E: h).

Xatv depletion affects endodermal specification

The modulation of induction processes by Xatv is also important in the specification of the normal endodermal territory. Previous reports failed to detect alterations in *endodermin* (*edd*) expression caused by Xlefty-MO injections (Branford and Yost, 2002). Gastrula stage *edd* expression marks axial mesoderm precursors as well as endoderm and, in the neurula, the notochord, prechordal plate, hatching gland, and entire endoderm, before becoming endoderm-specific at tailbud stages (Sasai et al., 1996). Below, we describe effects on *edd* expression that were detected at later stages in Xatv$^{MO1 + MO2}$-injected embryos (Figs. 6A: s–w). But, for this part of our gastrula stage analysis, we tried to select more rigorously endoderm-specific genes. We found that Xatv$^{MO1 + MO2}$ injection not only expanded the expression domain of *XSox17α*, an Xnr-responsive pan-endodermal marker (Hudson et al., 1997; Osada and Wright, 1999), but also increased the level of expression within this domain during gastrulation (Figs. 5A: a–f). Whole-mount in situ hybridization on bisected embryos showed that *XSox17α* expression was intensified and spatially expanded in the dorsal lip area (Figs. 5A: g, g′, h, h′). Dorsally, the expansion was dramatic in the superficial layer, while the ventral marginal zone showed expansion in both deep and superficial layers (Figs. 5A: g–h″). Another mesendodermal marker, expressed primarily in endoderm, *Mixer* (Henry and Melton, 1998), was also upregulated and expanded by Xatv$^{MO1 + MO2}$ during gastrulation (Figs. 5B: a–f) to form a broad marginal zone band of expression around the entire embryo. This expression was located in dorsal and ventral regions of bisected embryos in the superficial (endodermal) and deep (mesendodermal) layers (Figs. 5B: g–h″).

We conclude that mesendoderm specification is initiated relatively normally in Xatv-depleted embryos, with dorsoventral patterning still evident, but that loss of Xatv function leads to massive expansion of both dorsal/ventral mesodermal and endodermal markers, a significant degree of global dorsalization of the embryo, and an associated failure of the involution and convergence/extension movements of gastrulation.

Depletion of Xatv function expands mesodermal tissues during later embryogenesis

Above, we showed the importance of Xatv as a primary negative feedback regulator of the strength, duration, and range of Xnr signaling at early embryogenesis. Previously, Branford and Yost (2002) concluded that post-gastrula Xlefty-deficient exogastrulae exhibit a reversal of the A/P axis but relatively normal patterning of the mesoderm and endoderm. We found, however, that the Xatv functional knockdown was translated into a substantial effect on cell fate allocation in later embryos. While the hyperdorsalization of the Xatv$^{MO1 + MO2}$-injected embryos results in substantial death during or after gastrulation if kept in the vitelline membrane, 80–90% survive if the membrane is removed, allowing phenotypic evaluation at later stages. Since Xatv^{MO}-induced exogastrulation made it difficult to directly compare the differences of marker expression and tissue formation between uninjected and Xatv$^{MO1 + MO2}$-injected embryos, we decided to compare them to classical exogastrulae induced by high salt (HS-exogastrulae) as a control.

The pan-neural marker, *nrp-1* (Richter et al., 1988; Knecht et al., 1995), was expressed in the ectoderm (blue line) but not in the dorsal midline of the mesendodermal mass (yellow line) in both types of exogastrulae (Figs. 6A: a–c). Similarly, the expression of *cpl-1* and *Xkrox20*, markers for the dorsal forebrain and hindbrain, respectively (Knecht et al., 1995; Bradly et al., 1993), was detected in the expected pattern in the ectodermal part of the exogastrulae (data not shown). The expression of *Xotx2* was significantly upregulated in the mesendodermal tip of Xatv$^{MO1 + MO2}$-induced exogastrulae (white arrowheads; Figs. 6A: d–f). Although *Xotx2* is generally known as a marker for fore/midbrain at tailbud stage, prior to that it is expressed in the underlying prechordal mesendoderm, and is observed in the latter tissue in exogas-

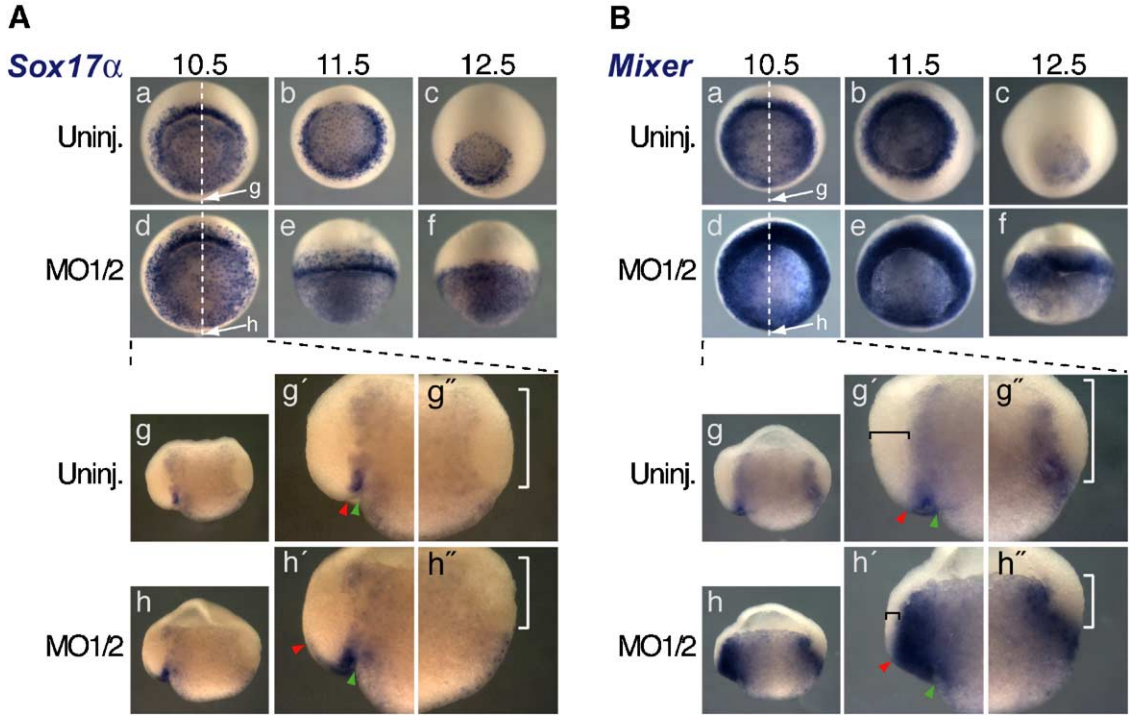

Fig. 5. Xatv is required for normal endoderm fate specification. (A) In situ hybridization with *Sox17α* in uninjected and Xatv$^{MO1 + MO2}$-injected embryos during gastrulation. (a–c) Uninjected embryos. (d–f) Xatv$^{MO1 + MO2}$-injected embryos. (a–d) Vegetal view, dorsal upwards. [Quantitative analysis of alterations shown: d, $n = 6/6$.] (e, f) Lateral view. [Quantitation: e, $n = 8/8$; f, $n = 9/10$.] (g, h) *Sox17α* expression at St. 10.5 detected by in situ hybridization after bisection through the center of the dorsal lip of (g) uninjected ($n = 10/10$) and (h) Xatv$^{MO1 + MO2}$-injected ($n = 9/10$) embryos (dorsal to the left). (g′, h′) Magnified views, dorsal side of panels g and h, compared to (g″, h″) magnified ventral side views. (B) *Mixer* expression in (a–c) uninjected and (d–f) Xatv$^{MO1 + MO2}$-injected embryos during gastrulation. (a–e) Vegetal view, dorsal to the top. [Quantitation: d, $n = 6/6$; e, $n = 8/8$.] (f) Lateral view ($n = 8/8$). (g, h) *Mixer* expression at St. 10.5 detected by in situ hybridization after bisection through the center of the dorsal lip of (g) uninjected ($n = 8/8$) and (h) Xatv$^{MO1 + MO2}$-injected ($n = 10/10$) embryos (dorsal to the left). (g′, h′) Magnified views, dorsal side of g and h compared to (g″, h″) magnified ventral views. Green arrowheads: dorsal lip. Red arrowheads: most animal/anterior expression limit of *Sox17α* (A) and *Mixer* (B). White brackets: separation of blastocoel floor from the edge of *Sox17α* (A) and *Mixer* (B) expression domains in the superficial layer. Black brackets: breadth of *Mixer*-negative area in the dorsal mesoderm region (B: g′, h′).

trulae (Blitz and Cho, 1995; Pannese et al., 1995). We conclude that there was substantial expansion of the prechordal mesoderm fate in Xatv$^{MO1 + MO2}$-induced exogastrulae. The increased width and intensity of midline expression, and substantial ectopic expression in the anterior mesendoderm tip (Figs. 8A: g–i, red arrowheads) of *Shh*, a marker of prechordal plate, floor plate, and notochord (Ruiz i Altaba et al., 1995; Ekker et al., 1995), also supported a large expansion of prechordal plate in Xatv$^{MO1 + MO2}$-induced exogastrulae. The midline expression of *Xatv* in normal embryos at these stages (Fig. 6A: j) primarily marks the neural tube floorplate (blue arrowhead) and hypochord (yellow arrowhead), with weaker notochord expression (Cheng et al., 2000). In HS-exogastrulae (Fig. 6A: k), the surface location and punctate signal for *Xatv* in the dorsal mesendodermal mass (yellow arrowhead) indicated the formation of hypochordal tissue, and an ectodermal *Xatv* signal was seen at the mesendodermal mass/ectoderm junction (blue arrowhead). *Xatv* expression in the dorsal mesendodermal mass was greatly upregulated and broader in Xatv$^{MO1 + MO2}$-induced exogastrulae (Fig. 6A: j–l′, recognizable as increased hypochordal tissue on the upper surface of the sections in Figs. 6B). The relative area of this (hypochord + notochord) tissue in transverse sections of Xatv$^{MO1 + MO2}$-induced exogastrulae (Figs. 6B: a–d) was more than two times larger than in HS-exogastrulae (Fig. 6B: e). Similarly, the expression of *MyoD*, a somitic mesoderm marker (Hopwood et al., 1989), was elevated and expanded (Figs. 6A: m–r). Quantitation of the total amount of mesodermal tissue, including somite and ventral mesoderm, in typical cross-sections from multiple embryos showed that it was approximately two-fold greater in Xatv$^{MO1 + MO2}$-induced exogastrulae compared to HS-induced ones (green dashed lines; Figs. 6B: a–d, f). In addition, histological analysis showed, within the mesodermal tissue in Xatv$^{MO1 + MO2}$-induced exogastrulae, a stack of layers of elongated cells with lozenge-shaped nuclei, indicative of differentiated somitic muscle (yellow dashed line; Fig. 6B: d); this tissue demarcation was less obvious in HS-exogastrulae. This somitic domain was determined from the residual *MyoD* signal on sections of embryos subjected to whole-mount in situ hybridization. Global endoderm formation between the two types of exogastrulae as marked by expression of *endodermin* (*edd;* Sasai et al., 1996) was similar in the two types of exogastrulae, being detected in the entire protruded mesendoderm (Figs. 6A: t–w). The Xatv$^{MO1 + MO2}$-induced exogastrulae, however, showed broad and strong *edd* staining in the midline, corresponding to the broad *Shh*-positive domain (yellow arrowheads; Fig. 6A: w). *edd* normally marks

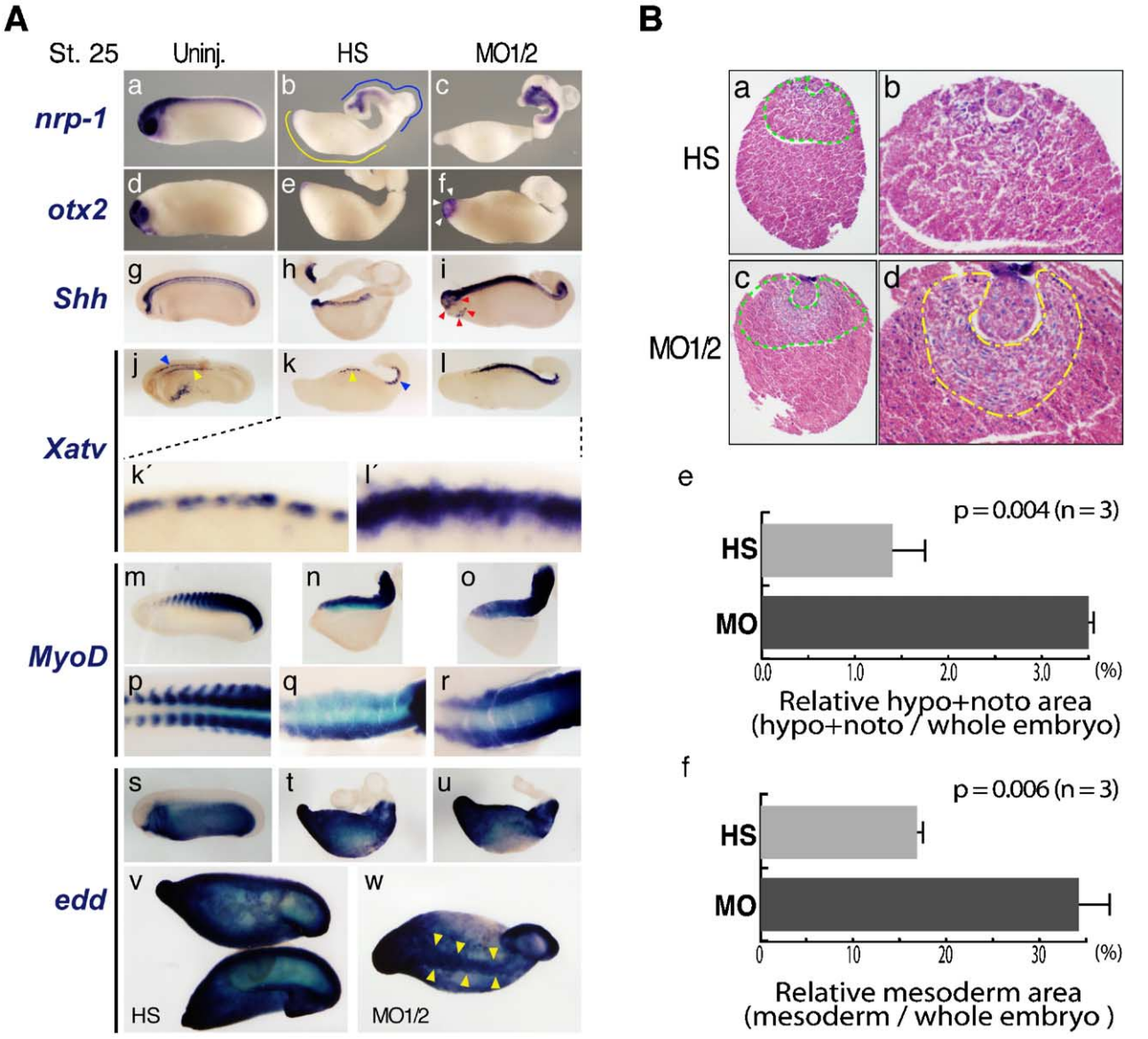

Fig. 6. Xatv is essential for proper formation of mesodermal tissues at later embryogenesis. Classical exogastrulae were induced by incubating embryos with high salt (HS) solution. Xatv$^{MO1 + MO2}$-injected embryos (30ng each) were incubated in 1× SS without vitelline membranes. When sibling embryos reached stage 25, exogastrulae were collected. (A) In situ hybridization. (a–c) *nrp-1* expression. [Quantitative analysis of alterations shown: b, $n = 4/5$; c, $n = 7/8$.] Yellow and blue lines in panel b indicate the protruded mesendodermal mass and ectoderm, respectively. (d–f) *Xotx2* expression. White arrowheads in panel f indicate the expanded prechordal plate in the anterior end. [Quantitation: e, $n = 5/5$; f, $n = 9/9$.] (g–i) *Shh* expression. Red arrowheads in panel i indicate the expanded prechordal plate in head mesoderm. [Quantitation: h, $n = 8/11$; i, $n = 14/18$.] (j–l) *Xatv* expression. [Quantitation: k, $n = 5/7$; f, $n = 10/15$.] Yellow and blue arrowheads in panel j: *Xatv* expression at the hypochord and neural tube floorplate, respectively. Yellow and blue arrowheads in panel k: *Xatv* signal at the dorsal mesendodermal mass and mesendodermal mass/ectoderm junction, respectively. (k′, l′) Magnified views of panels k and l, respectively. (m–r) *MyoD* expression. [Quantitation: n, $n = 6/6$; o, $n = 19/19$.] (s–w) *edd* expression. Yellow arrowheads in panel w indicate the intense staining in axial mesoderm. [Quantitation: t, $n = 9/9$; u, $n = 18/18$.] (a–o, s–u) Lateral views, anterior left, dorsal upward. (p–r) Magnified dorsal view of panels m–o, respectively. (v, w) Dorsal views. (B) Histological morphology and relative volume of notochord + hypochord and mesodermal tissues in HS and Xatv$^{MO1 + MO2}$-induced exogastrulae. (a–d) Hematoxylin/eosin staining of exogastrulae after transverse sectioning (after whole-mount in situ hybridization for *Xatv*). Green dashed lines in panels a and c encircle the mesoderm area including somite and ventral mesodermal cells. (b, d) Magnified views of dorsal side of panels a and c, respectively. Yellow dashed line in panel d indicates the crescent-shaped tissue containing elongated cells and nuclei that are indicative of somitic muscle differentiation, which is less obvious within somitic mesoderm area in the HS-induced exogastrulae. (e, f) Comparison of the relative volume of hypochord + notochord area (e) and mesodermal area (f) between HS- and Xatv$^{MO1 + MO2}$-induced exogastrulae.

the developing notochord in late neurula embryos (Sasai et al., 1996) and our analysis showed only weak *edd* expression in the notochord in both uninjected embryos and HS-exogastrulae at stage 25 (Figs. 6A: s, t, v). Therefore, it is likely that the axial-type *edd* expression detected in the Xatv-deficient exogastrulae reflects the increased notochord, with the failure to downregulate *edd* expression perhaps reflecting a delayed differentiation process. Overall, the elevated Xnr signaling during gastrulation in Xatv-deficient embryos leads to an increased allocation of cells towards prechordal mesoderm, notochord, hypochord, and other mesoderm fates such as somite and ventral mesoderm at later stages.

Increased range of Xnr signaling induces the expansion of Xbra expression

In Xatv$^{MO1 + MO2}$-injected embryos, the highly upregulated and expanded expression of Xnr-responsive genes, such as *Xbra* and *Xatv* itself, in the presence of intensified but only slightly expanded *Xnr1* and *Xnr2* expression suggests that Xnr ligands are inherently capable of long-range signaling in the very large *X. laevis* embryo. To test this hypothesis, we examined whether the expansions of the expression territories of the Nodal-responsive genes were blocked by inhibitors of Nodal signaling: the secreted Xnr-specific inhibitor, CerS, which directly binds Xnrs and inhibits signaling non-cell autonomously (Piccolo et al., 1999; Agius et al., 2000), and tALK4, a dominant-negative type I receptor that cell autonomously inhibits signaling by Nodal, Xnr1, Xnr2, Xnr4, and Activin (Reissmann et al., 2001). Xatv$^{MO1 + MO2}$ were injected into 1-cell stage embryos, which were then injected at the 32- to 64-cell stage in a single A- or B-tier blastomere (Moody, 1987) with *CerS* or *tALK4* RNA mixed with *β-galactosidase* (*β-gal*) RNA as lineage tracer. While the injection of *β-gal* RNA alone did not suppress the ectopic *Xbra* expression (Figs. 7B: a–c; n = 8/8), CerS produced from the labeled clone of cells gave rise to a marked patch of non-*Xbra*-expressing cells (Figs. 7B: d–f; n = 9/10). Because *CerS* is secreted, ectopic *Xbra* expression in Xatv$^{MO1 + MO2}$-injected embryos was inhibited in cells both within and away from the clone. When the injected clone was distributed to overlap the marginal region, tALK4 effectively blocked the endogenous *Xbra* expression domain in control embryos (Figs. 7A: d, d′; n = 7/7). The cell-autonomous tALK4 inhibitor blocked ectopic

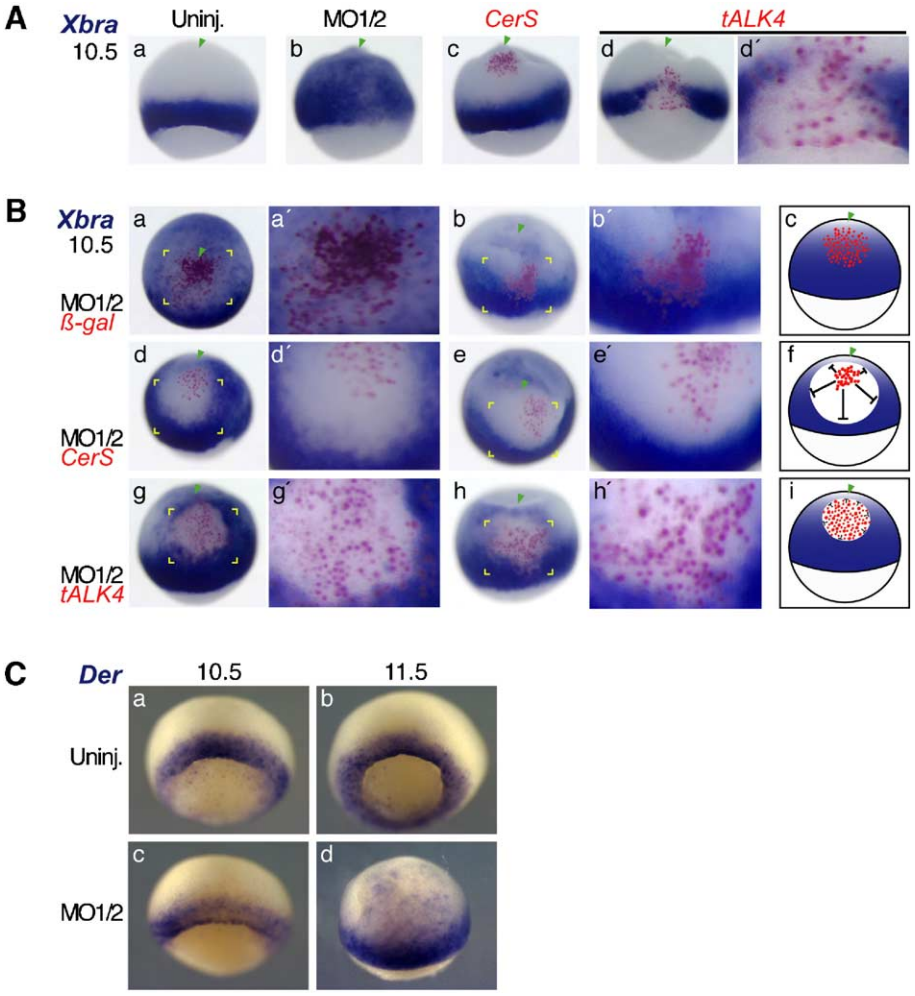

Fig. 7. Evidence for the expansion of *Xbra* expression by long-range Xnr signaling after Xatv knockdown. (A) In situ hybridization with *Xbra* on embryos at St. 10.5. (a) Uninjected embryo. (b) Xatv$^{MO1 + MO2}$-injected embryo. (c) *CerS*-injected embryos. (d) *tALK4*-injected embryo. (d′) High magnified view of panel d. (a–d) Lateral views. Red-gal staining in panels c and d detects the descendents of the cell injected with *CerS* and *tALK4*, respectively. (B) Xnr-specific inhibitors prevent ectopic *Xbra* expression in Xatv-deficient embryos. In situ hybridization on embryos at St. 10.5 detects *Xbra* expression, with red-gal staining detecting the descendants of the cell injected with RNA encoding the inhibitor (see text for detailed experimental design). Injection of *β-gal* (250 pg) does not affect ectopic *Xbra* expression (a–b′). CerS (500 pg) inhibits ectopic *Xbra* expression non-cell autonomously (d–e′), whereas tALK4 (500 pg) suppresses the ectopic *Xbra* expression cell autonomously (g–h′). (c, f, i) Simplified diagrams showing the effects on ectopic *Xbra* expression by *β-gal*, CerS, and tALK4, respectively. Red dots represent the clone of cells that express *β-gal*, CerS, and tALK4, respectively. "⊥" symbols in panels f and i show inhibition of Xnr signaling non-cell and cell autonomously by CerS and tALK4, respectively. (a, e) Animal views. (b, d, g, h) Lateral views skewed ~45° animal-ward. (a′, b′, d′, e′, g′, h′) Magnified views of the yellow bracketed area of panels a, b, d, e, g, and h, respectively. Green arrowheads in panels A and B indicate animal pole. (C) In situ hybridization with *Der* in (a, b) uninjected and (c, d) Xatv$^{MO1 + MO2}$-injected embryos. Dorsal views, with (d) angled downward slightly to visualize the animal-ward extent of *Der* signal.

Xbra expression only in lineage-labeled cells in Xatv$^{MO1 + MO2}$-injected embryos (Figs. 7B: g–i; n = 7/8). These data strongly suggest that the expanded *Xbra* (and other marker) expression in Xatv$^{MO1 + MO2}$-injected embryos was a direct result of an increased range of Xnr signaling associated with the intensified but only slightly expanded *Xnr1/2* expression domain.

Recent studies with overexpression and cleavage mutants of the TGFβ-related molecule Derrière (Der) have demonstrated transcriptional feedback loops and heterodimeric interactions between Xnrs and Der that may regulate mesoderm specification and patterning (Sun et al., 1999; Takahashi et al., 2000; Lee et al., 2001; Onuma et al., 2002; Eimon and Harland, 2002). We therefore examined how Xatv knockdown influences *Der* expression. The expression pattern of *Der* showed no noticeable alteration in Xatv$^{MO1 + MO2}$-injected embryos at stage 10.5, when *Xbra* expression has already expanded massively animal-wards (Fig. 7C: c; n = 21/26; Figs. 4D: g, j). At stage 11.5, however, *Der* expression became significantly expanded into the dorsal animal quadrant (Fig. 7C: d; n = 13/17). Because the expanded *Der* expression occurs after that of *Xbra*, we conclude that the dramatic expansion of *Xbra* expression in Xatv-deficient embryos is highly associated with elevated expression of *Xnrs* and the expansion of Xnr signaling, although there could be some interaction with Der (see Discussion).

Xatv and Xbra synergistically affect Xnr expression

The limited expansion of *Xnr2* expression in Xatv$^{MO1 + MO2}$-injected embryos, in the presence of a much broader response of other Xnr-responsive genes, suggested the existence of a remaining inhibitory influence blocking the Xnr autoregulatory loop. *Xbra* and *Xnr2* are normally expressed in mutually exclusive domains encircling the marginal zone of gastrulation stage embryos (Kumano and Smith, 2000; Eimon and Harland, 2002). Kumano et al. (2001) found that overexpressing *Xbra*

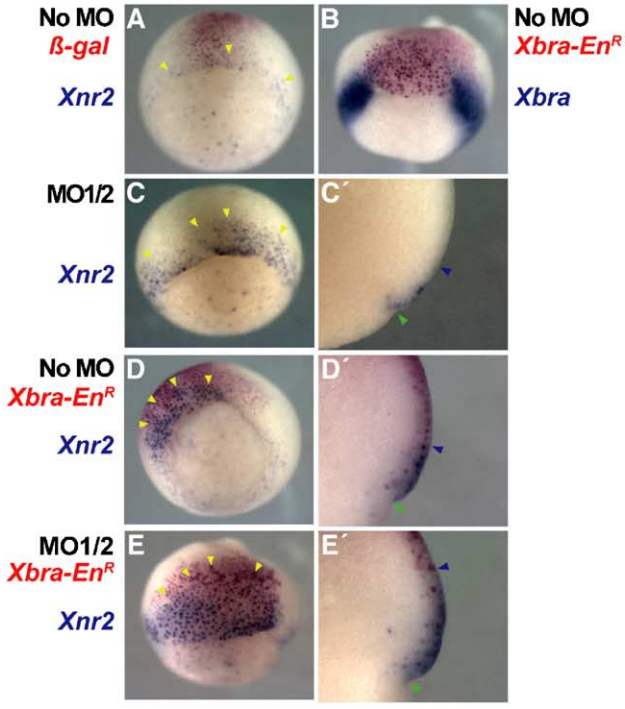

F

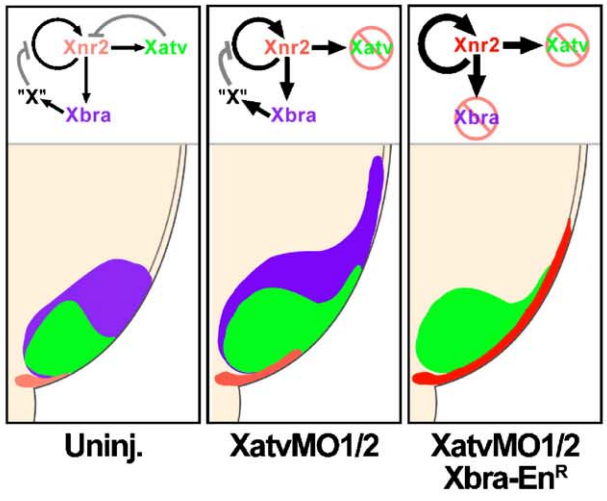

Fig. 8. Xatv and Xbra synergistically restrict the *Xnr* expression domain. *Xbra-En^R* RNA (1 ng) was injected ~45° above the equator into one blastomere of 4-cell stage embryos that previously received 30 ng each of (Xatv^{MO1} + Xatv^{MO2}) at the 1-cell stage. *β-gal* RNA (400 pg) was coinjected with *Xbra-En^R* RNA as lineage tracer. *Xnr2* and *Xbra* expression was analyzed by in situ hybridization at St. 10.5 after red-gal staining. (A) *Xnr2* expression, uninjected embryo. Red-gal staining indicates descendants of the *β-gal*-injected cell. (B) *Xbra* expression, *Xbra-En^R* RNA-injected embryo. (C) *Xnr2* expression, Xatv$^{MO1 + MO2}$-injected embryo. (D) *Xnr2* expression, *Xbra-En^R* RNA-injected embryo. (E) *Xnr2* expression, Xatv$^{MO1 + MO2}$ and *Xbra-En^R* RNA-injected embryo. (C′, D′, E′) Embryos bisected through the center of the *Xnr2* expression domain along animal-vegetal axis (from C, D and E). Green arrowheads, dorsal lip; blue arrowheads, anterior/animal boundary of *Xnr2* expression; yellow arrowheads in panels A, C, D, E—approximate animal limit of *Xnr2* expression domain. Note that *Xnr2* expression remains in the superficial layer. Black print: injection or uninjection of Xatv$^{MO1 + MO2}$ (MO1/2); red print: reagents coinjected with the *β-gal* lineage tracer, except (A); blue print: probes used for in situ hybridization. (F) Model of synergistic Xatv/Xlefty and Xbra-mediated restriction of *Xnr* expression during gastrulation. Schematic diagrams represent dorsal midline-bissected stage 10.5 early gastrulae, showing internal expression domains of *Xnr2* (red), *Xatv* (green), and *Xbra* (purple) in embryos that are (left) normal uninjected, (middle) Xatv/Xlefty MO1/MO2-coinjected, or (right) MO1/MO2 coinjected with Xbra-En^R. Increased line weight of arrows indicates elevated Xnr signaling, and increasing color intensity from light to dark red indicates increasing *Xnr2* expression intensity. In normal embryos, *Xnr2* expression is tightly restricted to the superficial layer of the dorsal lip (indentation), with Xnr–Xnr autoregulation maintaining this territory. *Xnr2* restriction is accomplished by both Xatv and Xbra, activated by Xnr signaling diffusing from the *Xnr2* expression domain. Primarily, Xatv inhibits *Xnr* expression non-cell autonomously. Xnr diffusing from producing cells activates expression of *Xbra* (purple) in both deep and superficial layers, which is stronger and earlier in the deep marginal zone compared to the superficial layer (see text). Rapid activation of *Xbra* provides an indirect repressive influence (Xbra is a transcriptional activator), implying that an unknown "Factor X" inhibits Xnr autoregulation, leading to the fixing of mutually exclusive expression domains for *Xnr2* and *Xbra*. Knockdown of Xatv function using *Xatv/Xlefty* MO1 + MO2 allows limited expansion of *Xnr2* expression, but elevated Xnr signaling range causes the massive expansion of *Xatv* and *Xbra* expression. *Xnr2* expression is still restricted by the increased Xbra-mediated indirect suppression. Interfering with both Xatv and Xbra allows expansion of *Xnr2* expression farther from the dorsal lip compared to either knockdown of Xatv or blocking Xbra function alone. Even in this condition, *Xnr2* expression occurs only in the superficial layer.

reduced *Xnr2* expression in the ventral marginal region, and that production of a dominant negative Xbra, Xbra-En^{R} (Conlon et al., 1996), expanded *Xnr2* expression in the same region. Because Xbra is a transcriptional activator, a simple model for the Xatv$^{MO1+MO2}$-injected embryos is that the broad expansion of Xbra results in the induction of a factor that then represses *Xnr* transcription. Consistent with this idea, we found that the use of Xbra-En^{R} to block Xbra function in Xatv$^{MO1+MO2}$-injected embryos led to a substantial expansion of the *Xnr* expression territory, much larger than in embryos receiving either Xbra-En^{R} or Xatv$^{MO1+MO2}$ alone. *Xbra-En^{R}* injection into control embryos prevented endogenous *Xbra* expression in both superficial and deep cells (Fig. 8B; n = 11/11; Supplemental Figs. 4B, B′, G, G′; data not shown), and produced a slight animal-ward expansion of superficial *Xnr2* expression during gastrulation (Figs. 8D, D′; n = 15/16; Supplemental Figs. 4D, D′, I, I′; also see Kumano et al., 2001). Notably, the intensity of the *Xnr2* signal in the expanded *Xnr2* expression domain was increased in the βgal-marked *Xbra-En^{R}*-expressing cells compared to uninjected or Xatv$^{MO1+MO2}$-injected embryos (Figs. 8A–D′). This difference was more evident when the intensity of *Xnr2* expression was compared without labeling the injected clone by β-gal expression, in which case *Xnr2* expression was detected as a punctate perinuclear signal (Supplemental Fig. 4). Production of Xbra-En^{R} in Xatv$^{MO1+MO2}$-injected embryos expanded the region that showed this higher signal intensity even farther animal-ward during gastrulation (Figs. 8E, E′; n = 28/31; Supplemental Figs. 4E, E′, J, J′). Some embryos receiving *Xbra-En^{R}* RNA, with or without previous Xatv$^{MO1+MO2}$ injection, showed strong *Xnr2* expression in cells laterally adjacent to βgal-marked cells (data not shown). This non-autonomous effect plausibly arises via increased Xnr secretion from Xbra-En^{R}-producing cells leading to the stimulation of *Xnr* expression in those adjacent cells.

An interesting observation here, however, was that despite the ability of the Xbra-En^{R} to work in deep and superficial cells as described above, the expanded *Xnr2* expression in all cases remained in the superficial cell layer, which is same layer selectivity shown by normal endogenous *Xnr2* expression (Figs. 8C′, D′, E′; Jones et al., 1995; Eimon and Harland, 2002). Collectively, these data suggest that *Xbra* expression acts as a potent strong indirect transcriptional influence on Xnr autoregulation, effectively blocking the expansion of *Xnr* transcription, but not the spreading of Xnr signals, in Xatv-deficient embryos. Xbra and Xatv therefore synergistically regulate Xnr autoregulation at the transcriptional and extracellular levels, respectively (Fig. 8F).

Discussion

We have produced evidence that the expression and range of action of Xnr in the *Xenopus* embryo are tightly regulated by Xatv-mediated blocking of the Xnr autoregulatory loop, and that the transient and restricted nature of expression is further assured by indirect Xbra-mediated transcriptional repression. These data are integrated into a model shown in Fig. 8F. In the absence of these negative regulatory influences, the induction of target genes of Xnr/activin-like signaling becomes massively expanded, in some cases (represented by *Xbra*, for example) being able to cover the entire animal cap. Such a huge expansion was not appreciated from the previous publications on Xatv interference, and likely reflects our concurrent targeting of both Xatv alloalleles via splicing and translation-blocking MOs, as discussed below. An interesting feature currently under study is the specific competence of the superficial layer to activate *Xnr* transcription, which was found both in normal embryos and in those in which the function of both Xatv and Xbra was reduced. Our findings extend significantly the previous findings on the knockdown of Xatv function in *Xenopus*, and increase our appreciation of the interaction and potency of extracellular Xatv and intracellular Xbra as regulators of Xnr induction during fate specification in *Xenopus*. At a general level, our results emphasize the degree to which, in all vertebrate embryos, the Nodal signaling pathway is under several layers of restrictive influence in order to limit its range in embryonic tissue, which can otherwise induce fate alterations very far from the ligand source.

Synergistic inhibition of Xatv function by Xatv^{A}- and Xatv^{B}-specific MOs

Recent studies injecting either of two different translation-blocking Xlefty/Xatv morpholinos concluded that Xlefty/Xatv spatially limits Nodal target gene expression, but in a fairly restricted fashion around the dorsal organizer domain (Branford and Yost, 2002; Tanegashima et al., 2004). The less dramatic effects compared to our findings may be related to targeting only *Xatv^{A}* or *Xatv^{B}*. Our translation-blocking Xatv^{MO1}, which matches 18 nucleotides of *Xatv^{B}*, did not inhibit *Xatv^{B}* mRNA translation in vitro (Fig. 1). Similarly, the *Xlefty*A- or *Xlefty*B-specific MOs of Branford and Yost (2002) had uninterrupted A-to-B, or B-to-A, cross-matches of only 11 and 16 nucleotides, respectively, thus reducing the likelihood of cross-copy knockdown. No results from coinjecting both of their MOs were reported. A general finding from our studies was that single MO injections were less effective at reducing Xatv function than mixtures of lower doses of MO that target Xatv^{A} and Xatv^{B} simultaneously (Fig. 2). The coinjection of splice blocker Xatv^{MO2} and translation blocker LeftyB-MO, which both target *Xatv^{B}*, was also less effective than simultaneously targeting *Xatv^{A}/Xatv^{B}* (Fig. 2A; Supplemental Fig. 1B). Overall, we conclude that more reproducible and stronger knockdown of Xatv function is achieved by synergistically inhibiting both Xatv^{A} and Xatv^{B} function.

Xatv and the strength and duration of Xnr signaling during gastrulation

Our analysis of Xatv-deficient embryos over several blastula/gastrula stages suggests a difference in the timing of negative feedback regulation by Lefty/Antivin on Nodal signaling between zebrafish and *Xenopus* embryos. In zebrafish, the upregulated and expanded expression of the *Xbra* homolog *ntl* was already present during blastula stages

(Agathon et al., 2001; Chen and Schier, 2002). In *Xenopus*, in contrast, *Xbra* and *Xatv* expression only became significantly different between control and Xatv$^{MO1 + MO2}$-injected embryos during mid-gastrula stage, concurrent with the dysregulation in *Xnr* expression (Figs. 3B, 4D; Supplemental Fig. 1A). Related to this observation, there are differences in normal frog and fish embryos in the spatiotemporal expression of *Lefty/antivin* expression. In zebrafish, *lefty/antivin* expression already encircles the margin during blastula stages (Thisse and Thisse, 1999; Bisgrove et al., 1999), while, in *Xenopus*, marginal zone *Xatv* expression is first robustly detected just at or prior to the onset of gastrulation (Cheng et al., 2000; Tanegashima et al., 2000). While the relevance of this temporal difference to the mechanisms of embryonic patterning in each species is not known, a conserved feature in both fish and frog embryos is that Lefty/Antivin-mediated negative feedback is essential during gastrulation for determining the appropriate level of Nodal signaling associated with cell fate specification and the differentiation of mesendodermal tissues at late embryogenesis (Fig. 6; Agathon et al., 2001).

Xatv and long-range signaling by Xnrs

Reduced Xatv function greatly expands the expression during gastrulation of markers of the organizer (*Gsc*, *Chd*, *ADMP*, *Cer*), mesoderm (*Xbra, XWnt8*), and endoderm (*Mixer*, *XSox17α*), as well as that of *Xatv* itself (Figs. 3B, 4, 5; Supplemental Fig. 3). Collectively, our results are consistent with the idea from the previous Xatv knockdown studies that germ layer specification and patterning require careful modulation of the extent of Xnr signaling. In normal embryos, Xnr signaling could occur via direct diffusion/transport of the ligand through embryonic tissue, although previous evidence argues both for and against Xnrs being long-range signals (Jones et al., 1996; White et al., 2002; Williams et al., 2004), or depend upon Xnr–Xnr autoactivation. The observation that *Xnr1* and *Xnr2* expression remains localized to the marginal zone, together with gross animal-ward expanded expression of target genes in Xatv-knockdown situations, is consistent with induction by long-range ligand signaling, as proposed for Sqt in zebrafish and Xnr2 in *Xenopus* (Chen and Schier, 2001; Williams et al., 2004). That the target genes are induced as a direct result of increased Xnr signaling is supported by the ability of the cell non-autonomous CerS and cell autonomous tALK4 Xnr-inhibitors to block the ectopic *Xbra* expression induced by Xatv$^{MO1 + MO2}$-injection (Fig. 7B). For both inhibitors, the *Xbra* expression detected outside the lineage-labeled (inhibitor-expressing) clone and on the side farthest away from the marginal *Xnr2* expression domain (Figs. 7B: d–i) fits with the concept that Xnr signaling is a very long-range influence in this large embryo. As compared to the direct diffusion of Xnr1 and Xnr2 from the equatorial region, it is also possible that a significant contribution towards the overall response of the embryo comes from the increased expression of the other mesoderm-inducing Xnrs, such as *Xnr4*, which is expressed in axial mesodermal tissue (Fig. 3m; Joseph and Melton, 1997).

Because mesendodermal specification and patterning involve an integrated response to many different signals, including Xnrs, Der, Wnts, BMPs – all having overlapping, dynamic, and interdependent spatiotemporal expression and functional characteristics that are still far from well understood – it is difficult to define how much the transcriptional response within embryonic tissues to reduced Xatv function is attributable only to specific inducers, i.e., the Nodal-related factors, or to which ones within this family. In other words, a key issue in these and other studies (Agius et al., 2000; Lee et al., 2001; Eimon and Harland, 2002; Howell et al., 2002) is how much the expanded expression of *Xbra* and additional Xnr target genes reflects increased Xnr signaling alone, or incorporates effects from inducers such as *Der*, which has a delayed but substantial expansion in Xatv$^{MO1 + MO2}$-injected embryos (Fig. 7C). Der may be particularly relevant here. It has been suggested to act as a relay inducer that maintains mesendoderm induction during late gastrulation/tailbud stages, principally to produce the posterior mesendoderm (Sun et al., 1999; White et al., 2002). Significant cross-activation between Xnrs and Der in overexpression assays (Takahashi et al., 2000; Lee et al., 2001; Onuma et al., 2002; Eimon and Harland, 2002), and the possibility of promiscuous ligand interactions (e.g., Osada and Wright, 1999; Yeo and Whitman, 2001; Eimon and Harland, 2002) complicate the dissection of inductive events from Xnr and Der in normal and Xatv knockdown situations. It is possible, for example, that the primary functional inducer in vivo is an Xnr–Der heterodimer, although it is also possible that such dimmers only form in the overexpression assays used so far.

An additional issue is the true specificity of CerS, which is currently thought to be Xnr-specific, but has been shown to inhibit the induction of *Der*, *Xbra*, and *Xnr1* expression by exogenous Der in animal cap assays (Eimon and Harland, 2002). The potential for significant cross-induction, however, makes it plausible that CerS is in fact an Xnr-specific inhibitor that does not physically interact with Der. We currently consider the early-expanded expression of target genes such as *Xbra*, *Xatv*, *Xwnt8*, and several organizer markers, to represent a response to signaling from Xnr and not Der. We base this conclusion upon: (1) Xnr and Der activate the formation of distinct transcriptional regulatory complexes, Fast1-containing ARF1 or Fast3-containing ARF2, respectively, at early and late gastrula stages. ARF1 and ARF2 have been independently linked to the different timing with which maximal Smad2 phosphorylation is induced by overexpressed Xnr (stage 9) or Der (stages 10–10.5: Lee et al., 2001; Howell et al., 2002). (2) Overexpression of Xnr1 or Xnr2 inhibits expression of *Fast3*, which normally begins during gastrulation (stages 10.25–11; Howell et al., 2002). The latter finding implies that extending the activity profile of Xnr signaling after Xatv knock-down (e.g., Figs. 3A: m) could shift *Fast3* expression even later, to mid-gastrulation, thereby minimizing the involvement of Der/ARF2 transcriptional responses in the early stage expansion of the mesendodermal territories. The Xnr–Der heterodimerization mentioned above, however, opens the possibility that Der may contribute to the expanded

expression of *Xbra* and other markers in Xatv-deficient embryos, even at St 10.5 when its expression level is similar to that in normal embryos (Fig. 7C). In addition, the Xnr–Der cross-inductive interactions raise the interesting question of why the apparently greatly increased Xnr signaling in Xatv-deficient embryos only increases *Der* expression during relatively late gastrulation stages, and why *Der* expression becomes broader only dorsally. More work is required to understand the interdependence of Xnr and Der expression and function in patterning. Nonetheless, the simplest inference is that the widespread ectopic expression of *Xbra* and other markers in early stage Xatv$^{MO1 + MO2}$-injected embryos is highly associated with an increased range of Xnr signaling, with maintenance of the ectopic gene expression domains and effects on tissue differentiation seen in later stage embryos resulting from cooperative induction by Xnrs and Der, whether they operate as homodimers or heterodimers.

Xatv regulates morphogenesis indirectly

Previous studies in zebrafish and mice showed that Lefty/antivin-deficiency enlarges the internalized mesoderm area in gastrula stage embryos (Meno et al., 1999; Feldman et al., 2002), as a result of excessive deep-cell internalization from an expanded germ ring and hypoblast (Feldman et al., 2002). The situation in *Xenopus* Xatv-deficient embryos seems somewhat different. The high level of Xnr signaling leads to substantial dorsalization and a failure to demarcate the future anterior–posterior zones properly with respect to each other, a situation incompatible with the production of concerted morphogenetic movements as defined by Ninomiya et al. (2004) (discussed in more detail below). In agreement with the data in Keller-type explant assays shown by Branford and Yost (2002), these defects lead to abrogated involution, mis-located convergence movements (Figs. 3B, 4A, B; Supplemental Figs. 3A–D), failure of blastopore closure, and exogastrulation. While our results basically agree with Branford and Yost (2002), we note significant differences between our embryos and theirs, which are perhaps also related to the greater reduction of Xatv function in our hands. For example, rather than remaining as distinct adjacent domains, we found extensive overlap of the expanded organizer (expressing *Gsc*, *Chd*, *ADMP*) and mesendoderm territories (both dorsal- and ventral-type; Figs. 4A, B, D; Supplemental Figs. 3E–L). The formation of a dorsal blastopore lip and subsequent blastopore groove in Xatv$^{MO1 + MO2}$-injected embryos implies the normal occurrence of the early gastrula-stage vegetal rotation that leads up to the first dorsal-side cell involutions (Winklbauer and Schürfeld, 1999). Normally, convergence forces in the marginal zone produce hoop stress around the blastopore that progressively closes the blastopore ventral-wards (Keller et al., 2000). Therefore, the failure to close the blastopore in Xatv$^{MO1 + MO2}$-injected embryos is probably directly related to the reduced cellular convergence in the marginal zone, associated with the long-lived, widespread, and overlapping expression domains of organizer markers.

Future work will address the detailed molecular and cell biological links between the large-scale repatterning of Xatv-deficient embryos and the misplaced convergence/extension movements. Xwnt11, the well-known regulator of the Wnt/planar cell polarity (Wnt/PCP) signaling pathway that is involved in convergence/extension, is a downstream target of Xbra (Heisenberg et al., 2000; Tada and Smith, 2000). Upregulated and shifted Xwnt11 activity in Xatv$^{MO1 + MO2}$-injected embryos could underlie the relocated morphogenetic movements if a broad supraphysiological level, rather than a normally graded amount, of Xwnt11 signaling in the marginal zone interferes with the generation of the vectorial information that underlies intercalatory tissue movements.

Linked to the latter concept is the idea that tissue movements caused by Wnt/PCP signaling are initiated in the vicinity of juxtaposed *Chd* and *Xbra* expression domains. Ninomiya et al. (2004) showed that convergent extension was initiated between conjugated animal caps that were previously treated separately with high or low activin doses. It also occurred in cell aggregates that had received a non-uniform activin signal ("graded explants"), in which counter-gradients of *Chd* and *Xbra* expression were established. In contrast, uniformly activin-treated explants with homogeneous *Chd* and *Xbra* expression did not undergo convergence/extension-based elongation. The latter condition mimics the overlapping *Chd*/*Xbra* expression that we observed at the dorsal marginal region of gastrulation-stage Xatv-deficient embryos (Fig. 4D; Supplemental Figs. 3C, D, J–L). The ideas of Ninomiya et al. (2004) allow an elaboration of the explanation offered by Branford and Yost (2002) for the exogastrulation of Xatv$^{MO1 + MO2}$-injected embryos: animal-ward relocation of the *Chd*–*Xbra* countergradient in Xatv knockdown embryos causes convergence extension movements to begin ectopically far above the dorsal marginal zone.

Superficial vs. deep induction of Xnr2 expression: role of Xbra suppression

Even when the inhibitory effects of Xatv and Xbra activity were blocked, the expanded *Xnr2* expression remained in the most superficial cell layer—the same layer specificity seen in normal embryos (Figs. 8C′, D′, E′; Jones et al., 1995; Eimon and Harland, 2002). This layer-specific induction of *Xnr2* expression is also obtained in animal caps that overexpress Xnr5 (S.T., M. Asashima and C.V.E.W.; submitted elsewhere), indicating a surprising level of control over the competence of the superficial vs. deep cells to respond to Nodal signaling. We consider this observation remarkable with respect to the traditional view of bilayered animal cap explants as comprising an inner sensorial-responsive layer and an outer cell layer that is refractory to induction. We are currently interested in characterizing the reason for this strict differential responsiveness, and note that Xnr3, which is primarily induced by Wnt signaling (McKendry et al., 1997; Hansen et al., 1997; Kofron et al., 2004), is also expressed in the superficial layer (Smith et al., 1995). That the expansion of expression in Xatv-deficient embryos of the endodermal marker *Xsox17α* occurs within the superficial (endoderm-fated) layer of the dorsal marginal zone (Figs. 5A: h, h′) may be linked to the observation that the

endodermal fate is specified by the highest levels of Nodal signaling, with these levels being reached in the cell layer expressing *Xnr1*/*Xnr2*.

There are two not necessarily mutually exclusive possibilities by which Xbra indirectly inhibits *Xnr2* transcription, and helps to restrict *Xnr2* expression to a narrow band of the superficial marginal zone. Both *Xnr1* and *Xnr2* are expressed in the blastopore-proximal region of the involuting marginal zone, supporting the notion of a primary role in inducing the formation of the head and/or anterior trunk. The narrowing of the marginal territory of *Xnr1/Xnr2* expression at mid-gastrula compared to preceding stages (Jones et al., 1995; Eimon and Harland, 2002) likely reflects the beginning of the involution of the blastopore lip-proximal superficial layer. The broad equatorial band of *Xbra* expression, which results from early-stage Xnr signaling (Agius et al., 2000), is separated from the blastopore lip by a gap equivalent to the width of the *Xnr2* expression domain (Kumano and Smith, 2000; Eimon and Harland, 2002). *Xbra* expression is strong in deep cells and much weaker in the superficial (future endoderm) layer. At the early gastrula stage, the *Xbra*-expressing cells approach the blastopore lip, and its expression level in the deep and superficial layers becomes more similar during mid-gastrulation (Vodicka and Gerhart, 1995; Eimon and Harland, 2002). Based on this architecture, Xbra could induce a suppressive signal from the deep cells that acts non-autonomously to inhibit *Xnr2* transcription within the adjacent superficial layer. In addition, Xbra produced in the prospective endoderm, perhaps more effectively when its expression becomes increased in this layer, could induce a cell autonomous suppressor. The failure to spread *Xnr2* expression inward to the deep marginal zone cells, while expanding significantly animalward, even when Xbra function is blocked in Xatv-deficient embryos, underscores the potential importance of the distinctive competence of the superficial layer to activate *Xnr2* expression. Other inducers, such as *Der*, which is expressed in deeper cells overlapping with *Xbra* expression, are not affected by these suppressive influences.

Acknowledgments

We thank Richard Harland, Hazel Sive, Daniel Kessler, William Smith, and Malcolm Moos for sharing reagents; Wright lab members for thoughtful comments on the experiments and the manuscript. We thank Yu Shyr for comments on statistical analysis. This work was supported by NIH grant number GM56238-08.

Appendix A. Supplementary data

Supplementary data associated with this article can be found in the online version at doi:10.1016/j.ydbio.2005.10.043.

References

Adachi, H., Saijoh, Y., Mochida, K., Ohishi, S., Hashiguchi, H., Hirao, A., Hamada, H., 1999. Determination of left/right asymmetric expression of nodal by a left side-specific enhancer with sequence similarity to a lefty-2. Genes Dev. 13, 1589–1600.

Agathon, A., Thisse, B., Thisse, C., 2001. Morpholino knock-down of Antivin1 and Antivin2 upregulates Nodal signaling. Genesis 30, 178–182.

Agius, E., Oelgeschläger, M., Wessely, O., Kemp, C., De Robertis, E.M., 2000. Endodermal Nodal-related signals and mesoderm induction in *Xenopus*. Development 127, 1173–1183.

Bisgrove, B.W., Essner, J.J., Yost, H.J., 1999. Regulation of midline development by antagonism of lefty and nodal signaling. Development 126, 3253–3262.

Blitz, I.L., Cho, K.W.Y., 1995. Anterior neuroectoderm is progressively induced during gastrulation: the role of the *Xenopus* homeobox gene orthodenticle. Development 121, 993–1004.

Bouwmeester, T., Kim, S-H., Sasai, Y., Lu, B., De Robertis, E.M., 1996. Cerberus is a head-inducing secreted factor expressed in the anterior endoderm of Spemann's organizer. Nature 382, 595–601.

Bradly, L.C., Snape, A., Bhatt, S., 1993. The structure and expression of the *Xenopus* Krox-20 gene: conserved and divergent pattern of expression in rhombomeres and neural crest. Mech. Dev. 40, 73–84.

Branford, W.W., Yost, H.J., 2002. Lefty-dependent inhibition of Nodal- and Wnt-responsive organizer gene expression is essential for normal gastrulation. Curr. Biol. 12, 2136–2141.

Branford, W.W., Essner, J.J., Yost, H.J., 2000. Regulation of gut and heart left–right asymmetry by context-dependent interactions between *Xenopus* lefty and BMP4 signaling. Dev. Biol. 223, 219–306.

Chang, C., Wilson, P.A., Mathews, L.S., Hemmati-Brivanlou, A., 1997. A *Xenopus* type I activin receptor mediates mesodermal but not neural specification during embryogenesis. Development 124, 827–837.

Chen, Y., Schier, AF., 2001. The zebrafish nodal signal squint functions as a morphogen. Nature 411, 607–610.

Chen, Y., Schier, A.F., 2002. Lefty proteins are long-range inhibitors of Squint-mediated Nodal signaling. Curr. Biol. 12, 2124–2128.

Chen, C., Shen, M.M., 2004. Two modes by which Lefty proteins inhibit Nodal signaling. Curr. Biol. 14, 618–624.

Cheng, A.M.S., Thisse, B., Thisse, C., Wright, C.V.E., 2000. The lefty-related factor Xatv acts as a feedback inhibitor of Nodal signaling in mesoderm induction and L-R axis development in *Xenopus*. Development 127, 1049–1061.

Cheng, S.K., Olale, F., Brivanlou, A.H., Schier, A.F., 2004. Lefty blocks a subset of TGFβ signals by antagonizing EGF-CFC coreceptors. PLoS Biol. 2, 0215–0226.

Cho, K.W.Y., Blumberg, B., Steinbeisser, H., De Robertis, E.M., 1991. Molecular nature of Spemann's organizer: the role of the *Xenopus* homeobox gene goosecoid. Cell 67, 1111–1120.

Christian, J.L., McMahon, J.A., McMahon, A.P., Moon, R.T., 1991. Xwnt-8, a *Xenopus* Wnt-1/int-1-related gene responsive to mesoderm-inducing growth factor, may play a role in ventral mesodermal patterning during embryogenesis. Development 111, 1045–1055.

Conlon, F.L., Sedgwick, S.G., Weston, K.M., Smith, J.C., 1996. Inhibition of Xbra transcription activation causes defects in mesodermal patterning and reveals autoregulation of Xbra in dorsal mesoderm. Development 122, 2427–2435.

Constam, D.B., Robertson, E.J., 1999. Regulation of bone morphogenetic protein activity by Pro domains and proprotein convertases. J. Cell Biol. 144, 139–149.

Eimon, P.M., Harland, R.M., 2002. Effects of heterodimerization and proteolytic processing on Derrière and Nodal activity: implications for mesoderm induction in *Xenopus*. Development 129, 3089–3103.

Ekker, S.C., McGrew, L.L., Lai, C.J., Lee, J.J., von Kessler, D.P., Moon, R.T., Beachy, P.A., 1995. Distinct expression and shared activities of members of the hedgehog gene family of *Xenopus laevis*. Development 121, 2337–2347.

Feldman, B., Concha, M.L., Saúde, L., Parsons, M.J., Adams, R.J., Wilson, S.W., Stemple, D.L., 2002. Lefty antagonism of Squint is essential for normal gastrulation. Curr. Biol. 12, 2129–2135.

Gierer, A., Meinhardt, H., 1972. A theory of biological pattern formation. Kybernetik 12, 30–39.

Hansen, C.S., Marion, C.D., Steele, K., George, S., Smith, W.C., 1997. Direct

neural induction and selective inhibition of mesoderm and epidermis inducers by Xnr3. Development 124, 483–492.
Heisenberg, C.P., Tada, M., Rauch, G.J., Saude, L., Concha, M.L., Geisler, R., Stemple, D.L., Smith, J.C., Wilson, S.W., 2000. Silberblick/Wnt11 mediates convergent extension movements during zebrafish gastrulation. Nature 405, 76–81.
Henry, G.L., Melton, D.A., 1998. Mixer, a homeobox gene required for endoderm development. Science 281, 91–96.
Hopwood, N.D., Pluck, A., Gurdon, J.B., 1989. MyoD expression in the forming somites is an early response to mesoderm induction in *Xenopus* embryos. EMBO J. 8, 3409–3417.
Howell, M., Inman, G.J., Hill, C.S., 2002. A novel *Xenopus* Smad-interacting forkhead transcription factor (XFast-3) cooperates with XFast-1 in regulating gastrulation movement. Development 129, 2823–2834.
Hudson, C., Clements, D., Friday, R.V., Stott, D., Woodland, H.R., 1997. Xsox17α and-β mediate endoderm formation in *Xenopus*. Cell 91, 397–405.
Ingham, P.W., McMahon, A.P., 2001. Hedgehog signaling in animal development: paradigms and principles. Genes Dev. 15, 3059–3087.
Jones, C.M., Kuehn, M.R., Hogan, B.L., Smith, J.C., Wright, C.V.E., 1995. Nodal-related signals induce axial mesoderm and dorsalize mesoderm during gastrulation. Development 121, 3651–3662.
Jones, C.M., Armes, N., Smith, J.C., 1996. Signaling by TGF-β family members: short-range effects of Xnr-2 and BMP-4 contrast with the long-range effects of activin. Curr. Biol. 6, 1447–1468.
Joseph, E.M., Melton, D.A., 1997. Xnr4: a *Xenopus* nodal-related gene expressed in the Spemann organizer. Dev. Biol. 184, 367–372.
Juan, H., Hamada, H., 2001. Roles of nodal-lefty regulatory loops in embryonic patterning of vertebrates. Genes Cells 6, 923–930.
Kay, B.K., Peng, H.B., 1991. *Xenopus laevis*: Practical Uses in Cell and Molecular Biology. Academic Press, San Diego.
Keller, R., Davidson, L., Edlund, A., Elul, T., Ezin, M., Shook, D., Skoglund, P., 2000. Mechanisms of convergence and extension by cell intercalation. Philos. Trans. R. Soc. London B355, 897–922.
Knecht, A.K., Good, P.J., Dawid, I.B., Harland, R.M., 1995. Dorsal–ventral patterning and differentiation of noggin-induced neural tissue in the absence of mesoderm. Development 121, 1927–1935.
Kofron, M., Puck, H., Standley, H., Wylie, C., Old, R., Whitman, M., Heasman, J., 2004. New roles for FoxH1 in patterning the early embryo. Development 131, 5065–5078.
Kumano, G., Smith, W.C., 2000. FGF restricts the primary blood islands to ventral mesoderm. Dev. Biol. 228, 304–314.
Kumano, G., Ezal, C., Smith, W.C., 2001. Boundaries and functional domains in the animal/vegetal axis of *Xenopus* gastrula mesoderm. Dev. Biol. 236, 465–477.
Le Good, J.A., Joubin, K., Giraldez, A.J., Ben-Haim, N., Beck, S., Chen, Y., Schier, A.F., Constam, D.B., 2005. Nodal stability determines signaling range. Curr. Biol. 15, 31–36.
Lee, M.A., Heasman, J., Whitman, M., 2001. Timing of endogenous activin-like signals and regional specification of the *Xenopus* embryo. Development 128, 2939–2952.
McKendry, R., Hsu, S.C., Harland, R.M., Grosschedl, R., 1997. LEF1/TCF proteins mediate wnt-inducible transcription from the *Xenopus* nodal-related 3 promoter. Dev. Biol. 192, 420–431.
Meinhardt, H., Gierer, A., 2000. Pattern formation by local self-activation and lateral inhibition. Bioessays 22, 753–760.
Meno, C., Saijoh, Y., Fujii, H., Ikeda, M., Yokoyama, T., Yokoyama, M., Toyoda, Y., Hamada, H., 1996. Left–right asymmetric expression of the TGFβ-family member lefty in mouse embryo. Nature 381, 151–155.
Meno, C., Ito, Y., Saijoh, Y., Matsuda, Y., Tashiro, K., Kuhara, S., Hamada, H., 1997. Two closely-related left–right asymmetrically expressed genes, lefty-1 and lefty-2: their distinct expression domains, chromosomal linkage and direct neuralizing activity in *Xenopus* embryos. Genes Cells 2, 513–524.
Meno, C., Gritsman, K., Ohishi, S., Ohfuji, Y., Heckscher, E., Mochida, K., Shimono, A., Kondoh, H., Talbot, W., Roberson, E.J., Schier, A.F., Hamada, H., 1999. Mouse lefty2 and zebrafish antivin are feedback inhibitors of nodal signaling during vertebrate gastrulation. Mol. Cell 4, 287–298.
Meno, C., Takeuchi, J., Sakuma, R., Koshiba-Takeuchi, K., Ohishi, S., Saijoh, Y., Miyazaki, J., Dijke, P.T., Ogura, T., Hamada, H., 2001. Diffusion of nodal signaling activity in the absence of the feedback inhibitor Lefty2. Dev. Cell 1, 127–138.
Moody, S.A., 1987. Fates of the blastomeres of the 32-cell-stage *Xenopus* embryo. Dev. Biol. 122, 300–319.
Moos, M., Wang, S., Krinks, M., 1995. Anti-dorsalizing morphogenetic protein is a novel TGF-(homolog expressed in the spemann organizer). Development 121, 4293–4301.
Nieuwkoop, P.D., Faber, J., 1967. Normal Table of *Xenopus laevis* (Daudin). North Hooland Publishing Company, Amsterdam.
Ninomiya, H., Elinson, R.P., Winklbauer, R., 2004. Antero-posterior tissue polarity links mesoderm convergent extension to axial patterning. Nature 430, 364–367.
Norris, D.P., Robertson, E.J., 1999. Asymmetric and node-specific nodal expression patterns are controlled by two distinct *cis*-acting regulatory elements. Genes Dev. 13, 1575–1588.
Onuma, Y., Takahashi, S., Yokota, C., Asashima, M., 2002. Multiple nodal-related genes act coordinately in *Xenopus* embryogenesis. Dev. Biol. 241, 94–105.
Osada, S.-I., Wright, C.V.E., 1999. *Xenopus* nodal-related signaling is essential for mesendodermal patterning during early embryogenesis. Development 126, 3229–3240.
Osada, S.-I., Saijoh, Y., Frisch, A., Yeo, C.-Y., Adachi, H., Watanabe, M., Whitman, M., Hamada, H., Wright, C.V.E., 2000. Activin/Nodal responsiveness and asymmetric expression of a *Xenopus* nodal-related gene converge on a FAST-regulated module in intron 1. Development 127, 2503–2514.
Pannese, M., Polo, C., Andreazzoli, M., Vignali, R., Kablar, B., Barsacchi, G., Boncinelli, E., 1995. The *Xenopus* homologue of otx2 is a maternal homeobox gene that demarcates and specifies anterior body regions. Development 121, 707–720.
Piccolo, S., Agius, E., Leyns, L., Bhattacharyya, S., Grunz, H., Bouwmeester, T., De Robertis, E.M., 1999. The head inducer Cerberus is a multifunctional antagonist of Nodal, BMP, and Wnt signals. Nature 397, 707–710.
Pogoda, H.-M., Solnica-Krezel, L., Driever, W., Meyer, D., 2000. The zebrafish forkhead transcription factor FoxH1/Fast1 is a modulator of Nodal signaling required for organizer formation. Curr. Biol. 10, 1041–1049.
Reissmann, E., Jörnvall, H., Blokzijl, A., Andersson, O., Chang, C., Minchiotti, G., Persico, M.G., Ibáñez, C.F., Brivanlou, A.H., 2001. The orphan receptor ALK7 and the activin receptor ALK4 mediate signaling by nodal proteins during vertebrate development. Genes Dev. 15, 2010–2022.
Rex, M., Hilton, E., Old, R., 2002. Multiple interactions between maternally-activated signaling pathways control *Xenopus* Nodal-related genes. Int. J. Dev. Biol. 46, 217–226.
Richter, K., Grunz, H., Dawid, I.B., 1988. Gene expression in the embryonic nervous system of *Xenopus laevis*. Proc. Natl. Acad. Sci. U. S. A. 85, 8068–8090.
Ruiz i Altaba, A., Jessell, T.M., Roelink, H., 1995. Restriction to floor plate induction by hedgehog and winged-helix genes in the neural tube of frog embryos. Mol. Cell. Neurosci. 6, 106–121.
Saijoh, Y., Adachi, H., Sakuma, R., Yeo, C.-Y., Yashiro, K., Watanabe, M., Hashiguchi, H., Mochida, K., Ohishi, S., Kawabata, M., Miyazono, K., Whitman, M., Hamada, H., 2000. Left–right asymmetric expression of lefty2 and nodal is induced by a signaling pathway that includes the transcription factor FAST2. Mol. Cell 5, 35–47.
Sakuma, R., Ohnishi, Y.Y., Meno, C., Fujii, H., Juan, H., Takeuchi, J., Ogura, T., Li, E., Miyazono, K., Hamada, H., 2002. Inhibition of Nodal signaling by Lefty mediated through interaction with common receptors and efficient diffusion. Genes Cells 7, 401–412.
Sasai, Y., Lu, B., Steinbeisser, H., Geissert, D., Gont, L.K., De Robertis, E.M., 1994. *Xenopus* chordin: a novel dorsalizing factor activated by organizer-specific homeobox genes. Cell 79, 779–790.
Sasai, Y., Lu, B., Piccolo, S., De Robertis, E.M., 1996. Endoderm induction by the organizer-secreted factors chordin and noggin in *Xenopus* animal caps. EMBO J. 15, 4547–4555.

Schier, A.F., 2003. Nodal signaling in vertebrate development. Annu. Rev. Cell Dev. Biol. 19, 589–621.

Schier, A.F., Shen, M.M., 1999. Nodal signaling in vertebrate development. Nature 403, 385–389.

Shen, M.M., Schier, A.F., 2000. The EGF-CFC gene family in vertebrate development. Trends Genet. 16, 303–309.

Sive, H.L., Gringer, R.M., Harland, R.M., 2000. Early Development of *Xenopus laevis*: A Laboratory Manual. Cold Spring Harbor Laboratory Press, Cold Spring Harbor, NY.

Smith, W.C., Harland, R.M., 1991. Injected Xwnt-8 RNA acts early in *Xenopus* embryos to promote formation of a ventral dorsalizing center. Cell 67, 753–765.

Smith, J.C., Price, B.M.J., Green, J.B.A., Weigel, D., Herrmann, B.G., 1991. Expression of a *Xenopus* homolog of Brachyury (T) is an immediate-early response to mesoderm induction. Cell 67, 79–87.

Smith, W.C., Mckendry, R., Ribish Jr., S., Harland, R.M., 1995. A nodal-related gene defines a physical and functional domain within the Spemann organizer. Cell 82, 37–46.

Sokol, S., Christian, J.L., Moon, R.T., Melton, D.A., 1991. Injected Wnt RNA induces a completed body axis in *Xenopus* embryos. Cell 67, 741–752.

Sun, B.I., Bush, S.M., Collins-Racie, L.A., LaVallie, E.R., DiBlasio-Smith, E.A., Wolfman, N.M., McCoy, J.M., Sive, H.L., 1999. derrière: a TGF-beta family member required for posterior development in *Xenopus*. Development 126, 1467–1482.

Tada, M., Smith, J.C., 2000. Xwnt11 is a target of *Xenopus* Brachyury: regulation of gastrulation movements via Dishevelled, but not through the canonical Wnt pathway. Development 12, 2227–2238.

Takahashi, S., Yokota, C., Takano, K., Tanegashima, K., Onuma, Y., Gato, J., Asashima, M., 2000. Two novel nodal-related genes initiate early inductive events in *Xenopus* Nieuwkoop center. Development 127, 5319–5329.

Tanegashima, K., Yokota, C., Takahashi, S., Asashima, M., 2000. Expression cloning of Xantivin, a *Xenopus* lefty/antivin-related gene, involved in the regulation of activin signaling during mesoderm induction. Mech. Dev. 99, 3–14.

Tanegashima, K., Haramoto, Y., Yokota, C., Takahashi, S., Asashima, M., 2004. Xantivin suppresses the activity of EGF-CFC genes to regulate nodal signaling. Int. J. Dev. Biol. 48, 275–283.

Taylor, M.F., Paulauskis, J.D., Wller, D.D, Kobzik, L., 1996. In vitro efficacy of morpholino-modified antisense oligomers directed against tumor necrosis factor-α mRNA. J. Biol. Chem. 271, 17445–17452.

Thisse, C., Thisse, B., 1999. Antivin, a novel and divergent member of the TGF (superfamily, negatively regulates mesoderm induction). Development 126, 229–240.

Tsuneizumi, K., Nakayama, T., Kamoshida, Y., Kornberg, T.B., Christian, J.L., Tabata, T., 1997. Daughters against dpp modulates dpp organizing activity in *Drosophila* wing development. Nature 389, 627–631.

Turing, A.M., 1952. The chemical basis of morphogenesis. Philos. Trans. R. Soc. London B237, 37–72.

Vodicka, M.A., Gerhart, J.C., 1995. Blastomere derivation and domains of gene expression in the Spemann Organizer of *Xenopus laevis*. Development 121, 3505–3518.

White, R.J., Sive, H.L., Smith, J.C., 2002. Direct and indirect regulation of derrière, a *Xenopus* mesoderm-inducing factor, by VegT. Development 129, 4867–4876.

Whitman, M., 2001. Nodal signaling in early vertebrate embryos: themes and variations. Dev. Cell 1, 605–617.

Williams, P.H., Hagemann, A., Gonzalez-Gaitan, M., Smith, J.C., 2004. Visualizing long-range movement of the morphogen Xnr2 in the *Xenopus* embryo. Curr. Biol. 14, 1916–1923.

Wilson, P.A., Melton, D.A., 1994. Mesodermal patterning by an inducer gradient depends on secondary cell–cell communication. Curr. Biol. 4, 676–686.

Winklbauer, R., Schürfeld, M., 1999. Vegetal rotation, a new gastrulation movement involved in the internalization of the mesoderm and endoderm in *Xenopus*. Development 126, 3703–3713.

Yang, J., Tan, C., Darken, R.S., Wilson, P.A., Klein, P.S., 2002. β-catenin/Tcf-regulated transcription prior to the midblastula transition. Development 129, 5743–5752.

Yeo, C., Whitman, M., 2001. Nodal signals to Smads through Cripto-dependent and Cripto-independent mechanisms. Mol. Cell 7, 949–957.